Multiple soil nutrient competition between plants, microbes, and mineral surfaces: Model development, parameterization, and example applications in several tropical forests

Qing Zhu[1*], William J. Riley[1], Jinyun Tang[1], Charles D. Koven[1]

[1] Climate Sciences Department, Earth Sciences Division, Lawrence Berkeley National Laboratory, Berkeley, CA 94720

[*] Correspondence to: Q. Zhu (qzhu@lbl.gov)

Abstract

Soil is a complex system where biotic (*e.g.*, plant roots, micro-organisms) and abiotic (*e.g.*, mineral surfaces) consumers compete for resources necessary for life (*e.g.*, nitrogen, phosphorus). This competition is ecologically significant, since it regulates the dynamics of soil nutrients and controls aboveground plant productivity. Here we develop, calibrate, and test a nutrient competition model that accounts for multiple soil nutrients interacting with multiple biotic and abiotic consumers. As applied here for tropical forests, the Nutrient COMpetition model (N-COM) includes three primary soil nutrients (NH_4^+, NO_3^-, and PO_x (representing the sum of PO_4^{3-}, HPO_4^{2-}, and $H_2PO_4^-$)) and five potential competitors (plant roots, decomposing microbes, nitrifiers, denitrifiers, and mineral surfaces). The competition is formulated with a quasi-steady-state chemical equilibrium approximation to account for substrate (multiple substrates share one consumer) and consumer (multiple consumers compete for one substrate) effects. N-COM successfully reproduced observed soil heterotrophic respiration, N_2O emissions, free phosphorus, sorbed phosphorus, and NH_4^+ pools at a tropical forest site (Tapajos). The overall model uncertainty was moderately well constrained. Our sensitivity analysis

revealed that soil nutrient competition was primarily regulated by consumer-substrate affinity rather than environmental factors such as soil temperature or soil moisture. Our results also imply that under strong nutrient limitation, relative competitiveness depends strongly on the competitor functional traits (affinity and nutrient carrier enzyme abundance). We then applied the N-COM model to analyze field nitrogen and phosphorus perturbation experiments in two tropical forest sites (in Hawaii and Puerto Rico) not used in model development or calibration. Under soil inorganic nitrogen and phosphorus elevated conditions, the model accurately replicated the experimentally observed competition among nutrient consumers. Although we used as many observations as we could obtain, more nutrient addition experiments in tropical systems would greatly benefit model testing and calibration. In summary, the N-COM model provides an ecologically consistent representation of nutrient competition appropriate for land BGC models integrated in Earth System Models.

1 Introduction

Atmospheric CO_2 concentrations have risen sharply since the pre-industrial era, primarily due to anthropogenic fossil fuel combustion and land use and land cover change [*Houghton*, 2003; *Le Quéré et al.*, 2013; *Marland et al.*, 2003]. Terrestrial ecosystems mitigate the increasing atmospheric CO_2 trend by absorbing roughly a quarter of anthropogenic CO_2 emissions [*Le Quéré et al.*, 2009]. However, it is still an open question whether the terrestrial CO_2 sink can be sustained [*Sokolov et al.*, 2008; *Zaehle et al.*, 2010], given that plant productivity is generally limited by soil nutrients [*Elser et al.*, 2007; *LeBauer and Treseder*, 2008; *Vitousek and Howarth*, 1991] and soil nutrients could be quickly depleted through biogeochemical [*Chauhan et al.*, 1981; *Nordin et al.*, 2001; *Shen et al.*, 2011] and hydrological [*Dise and Wright*, 1995; *Perakis and Hedin*, 2002] processes. Therefore, a holistic representation of soil nutrient dynamics is critically important to model the responses of terrestrial ecosystem CO_2 uptake to climate change.

Until recently, land models integrated in Earth System Models (ESMs) have largely ignored the close coupling between soil nutrient dynamics and the carbon cycle, although the impacts of soil nutrients (primarily Nitrogen and Phosphorus) regulating carbon-climate feedback are clearly required in ecosystem biogeochemistry and land models [*Zaehle and Dalmonech*, 2011; *Zhang et al.*, 2011]. For example, none of the land models in C^4MIP (Coupled Climate Carbon Cycle Model Intercomparison Project phase 4) had coupled Carbon and Nitrogen dynamics [*Friedlingstein et al.*, 2006]. The current generation of CMIP5 [*Anav et al.*, 2013] models used for the recent IPCC (Intergovernmental Panel on Climate Change) assessment had only two members (CLM4CN: *Thornton et al.* [2007]; and BNU-ESM: [*Ji et al.*, 2014]) that considered

nitrogen regulation of terrestrial carbon dynamics. However, as discussed below, several recent studies have shown that these models had large biases in most of the individual processes important for simulating nutrient dynamics. We therefore believe that, at the global scale, no credible representation of nutrient constraints on terrestrial carbon cycling yet exists in ESMs.

Further, none of the CMIP5 ESMs included a phosphorus cycle, which is likely important for tropical forest carbon budgets [*Vitousek and Sanford*, 1986]. The recent IPCC report highlights the importance of nitrogen and phosphorus availability on land carbon storage, even though the phosphorus limitation effect is uncertain [*Stocker et al.*, 2013]. Since the next generation of ESMs participating in the CMIP6 synthesis will continue to focus on the impacts of a changing climate on terrestrial CO_2 and abiotic exchanges with the atmosphere [*Provides*, 2014], developing ecologically realistic and observationally-constrained representations of soil nutrient dynamics and carbon-nutrient interactions in ESMs is critical.

The importance of nutrient limitations in terrestrial ecosystems has been widely demonstrated by nitrogen and phosphorus fertilization experiments [*Elser et al.*, 2007]. For instance, plant Net Primary Production (NPP) is enhanced in plots with nutrient addition [*LeBauer and Treseder*, 2008]. Similarly, plant growth can be stimulated due to atmospheric nitrogen deposition [*Matson et al.*, 2002]. Boreal forests are strongly limited by nitrogen availability [*Vitousek and Howarth*, 1991], because low temperatures reduce nitrogen mineralization [*Bonan and Cleve*, 1992] and N_2 fixation [*DeLuca et al.*, 2008; *DeLuca et al.*, 2002]. In contrast, tropical forests are often phosphorus limited [*Vitousek et al.*, 2010], since tropical soils are old and phosphorus derived from parent material

weathering has been depleted through long-term pedogenesis processes [*Vitousek and Farrington*, 1997; *Walker and Syers*, 1976]. In natural ecosystems without external nutrients inputs (*e.g.*, N deposition), soil nitrogen or phosphorus (or both) are likely insufficient to satisfy both plant and microorganism demands [*Vitousek and Farrington*, 1997]. Plants have to compete with microorganisms and mineral surfaces [*Kaye and Hart*, 1997; *Schimel et al.*, 1989] to obtain sufficient nutrients to sustain their biological processes (*e.g.*, photosynthesis, respiration). Therefore, it is critical to improve the representation of nutrient competition to accurately model how terrestrial ecosystems will respond to perturbations in soil nutrient dynamics (*e.g.*, from elevated nitrogen deposition or CO_2 fertilization-induced nutrient requirements).

Intense competition between plants and microorganisms is a well-observed phenomenon in nutrient-limited systems [*Hodge et al.*, 2000a; *Johnson*, 1992; *Kaye and Hart*, 1997]. Previously, plants were thought to be initial losers in nutrient competition, due to the fact that microbes are more intimately associated with substrates [*Woodmansee et al.*, 1981]. However, increasing observational evidence indicates that plants compete effectively with soil microorganisms [*Schimel and Bennett*, 2004] under certain circumstances; sometime even outcompeting them and suppressing microbial growth [*Hu et al.*, 2001; *J Wang and Lars*, 1997]. ^{15}N isotope studies have also demonstrated that plants can capture a large fraction of added nitrogen [*Hodge et al.*, 2000b; *Marion et al.*, 1982]. In the short term (days to months), plants maintain their competitiveness mainly through (1) establishing mycorrhizal fungi associations [*Drake et al.*, 2011; *Rillig et al.*, 1998], which help plants acquire organic and inorganic forms of nitrogen [*Hobbie and Hobbie*, 2006; *Hodge and Fitter*, 2010] and (2) root exudation of extracellular enzymes

106 that decompose rhizosphere soil organic matter [*Phillips et al.*, 2011]. In the relatively
107 longer term (months to years), morphological adjustment occurs; for example, plants
108 allocate more carbon to fine roots to explore laterally and deeper [*Iversen et al.*, 2011;
109 *Jackson et al.*, 2009]. Finally, over the course of years to decades, plant succession can
110 occur [*Medvigy et al.*, 2009; *Moorcroft et al.*, 2001] and the new plant demography will
111 need to be considered to represent nutrient controls on this time scale.
112 Given these patterns from the observational literature, nutrient competition is
113 either absent or over-simplified in existing Earth System Models (ESMs). One common
114 representation of plant-microbe competition is that plants compete poorly against
115 microbes in resource acquisition. For example, the O-CN land model [*Zaehle and Friend*,
116 2010] assumes that soil decomposing microbes have the priority to immobilize soil
117 mineral nitrogen. After microbes meet their demands, the remaining nitrogen is then
118 available for plant uptake.
119 Another treatment in ESM land models is that microbial and plant nutrient
120 acquisition competitiveness is based on their relative demands. For example, CLM4CN
121 [*Thornton et al.*, 2007] assumes that the plant and microbial nitrogen demands are
122 satisfied simultaneously. Under nitrogen infertile conditions, all nitrogen demands in the
123 system are down-regulated proportional to the individual demands and subject to
124 available soil mineral nitrogen. This approach led to unrealistic diurnal cycles of gross
125 primary production (GPP), with midday depressions in GPP occurring because of
126 predicted diurnal depletion of the soil mineral nitrogen pool. Emergent impacts of this
127 conceptualization of nutrient constraints on GPP resulted in poor predictions compared to
128 observations, with smaller than observed plant C growth responses to N deposition

129 [*Thomas et al.*, 2013a] and larger than observed responses to N fertilization [*Thomas et*
130 *al.*, 2013b]. Further, most biogeochemistry models not integrated in ESMs also adopt one
131 of these approaches. For instance, Biome-BGC [*Running and Coughlan*, 1988],
132 CENTURY [*Parton et al.*, 1988], CASA (Carnegie-Ames-Stanford Approach; [*Potter et*
133 *al.*, 1993]) and the Terrestrial Ecosystem Model - TEM [*McGuire et al.*, 1992] assume
134 that available nutrients preferentially satisfy the soil microbial immobilization demand.
135 We believe the two conceptualizations of competition used in ESMs substantially
136 over-simplify competitive interactions between plants and microbes and lead to biases in
137 carbon cycle predictions. To begin to address the problems with these simplified
138 approaches, Tang and Riley (2013) showed that complex consumer-substrate networks
139 can be represented with an approach (called Equilibrium Chemical Approximation (ECA)
140 kinetics) that simultaneously resolves multiple demands for multiple substrates, and
141 demonstrated that the approach was consistent with observed litter decomposition
142 observations. ECA kinetics has also recently been applied to analyze the emergent
143 temperature response of SOM decomposition, considering equilibrium, non-equilibrium,
144 and enzyme temperature sensitivities and abiotic interactions with mineral surfaces [*Tang*
145 *and Riley*, 2014]. We extend on that work here by presenting an implementation of ECA
146 kinetics to represent competition for multiple soil nutrients in a multiple consumer
147 environment. We note that this paper demonstrates a method to handle instantaneous
148 competition in the complex soil-plant network, but a robust competition representation
149 for climate-scale models will require representation of dynamic changes in plant
150 allocation and plant composition.

The aim of this study is to provide a reliable nutrient competition approach applicable for land models integrated in ESMs. However, before integration into an ESM, the competition model needs to be carefully calibrated and independently tested against observational data. This paper will therefore focus on model development and evaluation at several tropical forest sites where observations are available. Our objectives are to: (1) develop a soil biogeochemistry model with multiple nutrients (*i.e.*, NH_4^+, NO_3^-, and PO_x (represented as the sum of PO_4^{3-}, HPO_4^{2-}, and $H_2PO_4^-$)) and multiple nutrient consumers (*i.e.*, decomposing microbes, plants, nitrifiers, denitrifiers, and mineral surfaces) competition using ECA kinetics [*Tang and Riley*, 2013; *Zhu and Riley*, 2015]; (2) constrain the model with *in situ* observational datasets of soil carbon, nitrogen, and phosphorus dynamics using a Markov Chain Monte Carlo (MCMC) approach; and (3) test model performance against nitrogen and phosphorus fertilization studies.

2 Method

2.1 Model development

The Nutrient COMpetition model (N-COM) is designed as a soil biogeochemistry model (Figure 1) to simulate soil carbon decomposition, nitrogen and phosphorus transformations, abiotic interactions, and plant demands. Although our ultimate goal is to incorporate N-COM into a decomposition model that represents active microbial activity as the primary driver of decomposition, we start here by presenting the N-COM approach using a Century-like [*Koven et al.*, 2013; *Parton et al.*, 1988] structure, with additions to account for phosphorus dynamics. In our approach, we calculate potential immobilization using literature-derived parameters (*e.g.*, *VMAX*, K_M) in a Michaelis-Menten (MM) kinetics framework. The potential immobilization is subsequently modified using the ECA competition method.

Five pools of soil organic Carbon (C), Nitrogen (N), and Phosphorus (P) are considered: Coarse Wood Debris (CWD), litter, fast Soil Organic Matter (SOM) pool, medium SOM pool, and slow SOM pool. Litter is further divided into three sub-groups: metabolic, cellulose, and lignin. The soil organic C, N, and P decomposition ($F_{C,j}^{dec}$, $F_{N,j}^{dec}$, $F_{P,j}^{dec}$) follow first-order decay:

$$F_{C,j}^{dec} = k_j C_j r_\theta r_T \quad (1)$$

$$F_{N,j}^{dec} = k_j N_j r_\theta r_T \quad (2)$$

$$F_{P,j}^{dec} = k_j P_j r_\theta r_T \quad (3)$$

where k_j is the rate constant of soil organic matter decay (s^{-1}); C_j, N_j, and P_j are pool sizes ($g\ m^{-2}$) of carbon, nitrogen, and phosphorus, respectively (*j* from 1 to 7 represents the soil organic matter pools: CWD, metabolic litter, cellulose litter, lignin litter, fast

SOC, median SOC, slow SOC); r_T and r_θ (dimensionless) are soil temperature and moisture environmental regulators.

Decomposed carbon ($F_{C,i}^{dec}$) (upstream i^{th} pool) either (1) enters a downstream pool (j^{th}) or (2) is lost as CO_2. Soil organic carbon (downstream j^{th} pool) temporal change is calculated as:

$$\frac{dC_j}{dt} = -F_{C,j}^{dec} + \sum_{i=1}^{N} F_{C,ij}^{move} \quad (4)$$

where $\sum_{i=1}^{N} F_{C,ij}^{move}$ is the summation of carbon fluxes that move from the upstream pool (i) to the downstream pool (j) due to the decomposition of upstream SOC. For each upstream carbon pool (i = *1, 2, ..., 7*), the fractions integrated into downstream pools (j = *1, 2, ..., 7*) is summarized in a 7×7 matrix f_{ij} (Table 2). The percentage of decomposed carbon that is respired as CO_2 is represented by g_i (Table 2). Simultaneously, soil organic N and P changes follow C decomposition:

$$\frac{dN_j}{dt} = -F_{N,j}^{dec} + \sum_{i=1}^{N} F_{N,ij}^{move} + \sum_{i=1}^{N} F_{NH4,ij}^{immob} + \sum_{i=1}^{N} F_{NO3,ij}^{immob} \quad (5)$$

$$\frac{dP_j}{dt} = -F_{P,j}^{dec} + \sum_{i=1}^{N} F_{P,ij}^{move} + \sum_{i=1}^{N} F_{P,ij}^{immob} \quad (6)$$

where $F_{N,ij}^{move}$ and $F_{P,ij}^{move}$ are fluxes of nitrogen and phosphorus moving from the upstream (i) to downstream (j) pools. $F_{NH4,ij}^{immob}$, $F_{NO3,ij}^{immob}$, and $F_{P.ij}^{immob}$ are immobilization fluxes of soil mineral nitrogen and phosphorus. $F_{N,j}^{dec}$ and $F_{P,j}^{dec}$ represent soil organic matter decomposition losses.

Equations (5) and (6) state that changes in the j^{th} organic N or P pool are the summation of three terms: (1) organic N and P lost during soil organic matter mineralization ($-F_{N,j}^{dec}$ and $-F_{P,j}^{dec}$); (2) a fraction of the i^{th} organic N or P pool (upstream) enters into the j^{th} pool (downstream) ($F_{N,ij}^{move}$ and $F_{P,ij}^{move}$); and (3) soil microbial immobilization ($F_{NH4,ij}^{immob}$, $F_{NO3,ij}^{immob}$, and $F_{P,ij}^{immob}$). Immobilization occurs only when the newly entering organic N is insufficient to sustain the soil C:N (or C:P) ratio (more details described in Appendix A).

The inorganic nitrogen pools (NH_4^+ and NO_3^- (Eqn. 7 -8)) are altered by production (organic N mobilized by microbes), consumption (uptake by plants and microbes, gaseous or aqueous losses), and transformation (nitrification and denitrification). Inorganic P (PO_x) is assumed to be either taken up by plants and decomposing microbes or adsorbed to mineral surfaces (Eqn. 9). Plants utilize all forms of phosphate (*e.g.*, PO_4^{3-}, HPO_4^{2-}, and $H_2PO_4^-$), but for simplicity we use the symbol PO_x to represent the sum of all possible phosphate forms throughout the paper.

$$\frac{d[NH4]}{dt} = \sum_{j=1}^{N}\sum_{i=1}^{N} F_{NH4,ij}^{mob} - F_{NH4}^{nit} - F_{NH4}^{plant} - F_{NH4}^{immob} + F^{BNF} + F_{NH4}^{dep} \quad (7)$$

$$\frac{d[NO3]}{dt} = -F_{NO3}^{den} + (1 - f^{N2O})F_{NH4}^{nit} - F_{NO3}^{plant} - F_{NO3}^{immob} - F_{NO3}^{leach} + F_{NO3}^{dep} \quad (8)$$

$$\frac{d[PO_x]}{dt} = \sum_{j=1}^{N}\sum_{i=1}^{N} F_{P,ij}^{mob} - F_{P}^{plant} - F_{P}^{immob} - F_{P}^{surf} - F_{P}^{leach} + F^{weather} \quad (9)$$

where $F_{NH4,ij}^{mob}$ and $F_{P,ij}^{mob}$ are gross mineralization rates for nitrogen and phosphorus. F_{NH4}^{nit} is the nitrification flux, part of which is lost through a gaseous pathway (f^{N2O}) and the rest is incorporated into the NO_3^- pool. F_{NO3}^{den} is the denitrification flux, which transforms nitrate to N_2O and N_2 which then leave the soil system. Plant uptake of soil NH_4^+, NO_3^-,

and PO_x are represented as F_{NH4}^{plant}, F_{NO3}^{plant}, and F_P^{plant}, respectively. Soil decomposing microbial immobilization of soil NH_4^+, NO_3^-, and PO_x are represented as F_{NH4}^{immob}, F_{NO3}^{immob}, and F_P^{immob}. F_{NO3}^{leach}, and F_P^{leach} are leaching losses of soil NO_3^- and PO_x. External inputs into soil inorganic N pools include atmospheric ammonia deposition (F_{NH4}^{dep}), atmospheric nitrate deposition (F_{NO3}^{dep}), and biological nitrogen fixation (F^{BNF}). External sources of phosphate come from parent material weathering ($F^{weather}$).

Finally, the dynamics of sorbed P (P_S), occluded P (P_O), and parent material P (P_P) are modeled as:

$$\frac{d[P_S]}{dt} = F_P^{surf} - F_P^{occl} \quad (10)$$

$$\frac{d[P_O]}{dt} = F_P^{occl} \quad (11)$$

$$\frac{d[P_P]}{dt} = -F^{weather} + F_P^{dep} \quad (12)$$

where the pool of sorbed P is balanced by the adsorption flux (F_P^{surf}) and occlusion flux (F_P^{occl}). Parent material is lost by weathering ($F^{weather}$) and is slowly replenished by external atmospheric phosphorus inputs (F_P^{dep}, such as dust). More detailed information on the modeled C, N, and P fluxes is documented in Appendix A.

2.2 Multiple-consumer-multiple-resource competition network

The soil biogeochemistry model presented in **section 2.1** has multiple potential nutrient consumers (plants, SOM decomposing microbes, nitrifiers, denitrifiers, mineral surfaces) and multiple soil nutrients (NH_4^+, NO_3^-, PO_x). The consumer-resource network is summarized in Table 1. As in many land BGC models (CLM, Century, *etc.*), we have

not explicitly included the mineral surface adsorptions of NH_4^+ and NO_3^-, since we assume ammonia is quickly protected by mineral surfaces from leaching (no leaching term in Eqn. 7) but then released for plant and microbial uptake when the biotic demand arises. An improved treatment of these dynamics would necessitate a prognostic model for pH, which is beyond the scope of this analysis. Unlike sorbed P (which can be occluded), there is no further abiotic loss of sorbed ammonia. Therefore, the free ammonia pool is interpreted in the current model structure as a potential free ammonia pool (free + sorbed).

Competition between different consumers in acquiring different resources is summarized in Table 1. Each consumer-substrate competition reaction is represented by:

$$S + E \underset{k_1^-}{\overset{k_1^+}{\rightleftharpoons}} C \xrightarrow{k_2^+} P + E \tag{13}$$

The enzyme (*E: e.g., nutrient carrier enzyme produced by plants and microbes*) and substrate (*S: e.g., NH_4^+, NO_3^-*) reaction (reversible reaction) forms a substrate-enzyme complex (*C*). The following irreversible reaction leads to product (*P: meaning the nutrients has been taken up*) and releases enzyme (*E*) back into soil media. For the whole complex reaction network, nutrient uptakes are formulated as:

$$F_{NH4}^{plant} = k_{NH4}^{plant} \cdot \frac{[NH4] \cdot [E_N^{plant}]}{K_M^{plant,NH4}\left(1 + \underbrace{\frac{[NH4]}{K_M^{plant,NH4}}}_{(1)} + \underbrace{\frac{[NO3]}{K_M^{plant,NO3}}}_{(2)} + \underbrace{\frac{[E_N^{plant}]}{K_M^{plant,NH4}}}_{(3)} + \underbrace{\frac{[E_N^{mic}]}{K_M^{mic,NH4}}}_{(4)} + \underbrace{\frac{[E_N^{nit}]}{K_M^{nit,NH4}}}_{(5)}\right)} \tag{14}$$

$$F_{NH4}^{immob} = k_{NH4}^{immob} \cdot \frac{[NH4] \cdot [E_N^{mic}]}{K_M^{mic,NH4}\left(1 + \frac{[NH4]}{K_M^{mic,NH4}} + \frac{[NO3]}{K_M^{mic,NO3}} + \frac{[E_N^{plant}]}{K_M^{plant,NH4}} + \frac{[E_N^{mic}]}{K_M^{mic,NH4}} + \frac{[E_N^{nit}]}{K_M^{nit,NH4}}\right)} \tag{15}$$

$$F_{NH4}^{nit} = k_{NH4}^{nit} \cdot \frac{[NH4] \cdot [E_{NH4}^{nit}]}{K_M^{nit,NH4}\left(1 + \frac{[NH4]}{K_M^{nit,NH4}} + \frac{[E_N^{plant}]}{K_M^{plant,NH4}} + \frac{[E_N^{mic}]}{K_M^{mic,NH4}} + \frac{[E_N^{nit}]}{K_M^{nit,NH4}}\right)} \tag{16}$$

$$F_{NO3}^{plant} = k_{NO3}^{plant} \cdot \frac{[NO3] \cdot [E_N^{plant}]}{K_M^{plant,NO3}(1 + \frac{[NH4]}{K_M^{plant,NH4}} + \frac{[NO3]}{K_M^{plant,NO3}} + \frac{[E_N^{plant}]}{K_M^{plant,NO3}} + \frac{[E_N^{mic}]}{K_M^{mic,NO3}} + \frac{[E_N^{den}]}{K_M^{den,NO3}})} \quad (17)$$

$$F_{NO3}^{immob} = k_{NO3}^{immob} \cdot \frac{[NO3] \cdot [E_N^{mic}]}{K_M^{mic,NO3}(1 + \frac{[NH4]}{K_M^{mic,NH4}} + \frac{[NO3]}{K_M^{mic,NO3}} + \frac{[E_N^{plant}]}{K_M^{plant,NO3}} + \frac{[E_N^{mic}]}{K_M^{mic,NO3}} + \frac{[E_N^{den}]}{K_M^{den,NO3}})} \quad (18)$$

$$F_{NO3}^{den} = k_{NO3}^{den} \cdot \frac{[NO3] \cdot [E_{NO3}^{den}]}{K_M^{den,NO3}(1 + \frac{[NO3]}{K_M^{den,NO3}} + \frac{[E_N^{plant}]}{K_M^{plant,NO3}} + \frac{[E_N^{mic}]}{K_M^{mic,NO3}} + \frac{[E_N^{den}]}{K_M^{den,NO3}})} \quad (19)$$

$$F_P^{plant} = k_P^{plant} \cdot \frac{[PO_x] \cdot [E_P^{plant}]}{K_M^{plant,P}(1 + \frac{[PO_x]}{K_M^{plant,P}} + \frac{[E_P^{plant}]}{K_M^{plant,P}} + \frac{[E_P^{mic}]}{K_M^{mic,P}} + \frac{[E_P^{surf}]}{K_M^{surf,P}})} \quad (20)$$

$$F_P^{mic} = k_P^{mic} \cdot \frac{[PO_x] \cdot [E_P^{mic}]}{K_M^{mic,P}(1 + \frac{[PO_x]}{K_M^{mic,P}} + \frac{[E_P^{plant}]}{K_M^{plant,P}} + \frac{[E_P^{mic}]}{K_M^{mic,P}} + \frac{[E_P^{surf}]}{K_M^{surf,P}})} \quad (21)$$

$$F_P^{surf} = k_P^{surf} \cdot \frac{[PO_x] \cdot [E_P^{mic}]}{K_M^{surf,P}(1 + \frac{[PO_x]}{K_M^{surf,P}} + \frac{[E_P^{plant}]}{K_M^{plant,P}} + \frac{[E_P^{mic}]}{K_M^{mic,P}} + \frac{[E_P^{surf}]}{K_M^{surf,P}})} \quad (22)$$

where F represent the nutrient uptake fluxes and k is the base reaction rate that enzyme-substrate complex forms product (k_2^+ in Eqn. 13). $[E]$ and K_M denote enzyme abundance and half saturation constants (substrate-enzyme affinity). Superscripts and subscripts refer to consumers and substrates, respectively. These equations account for the effect of (1) multiple substrates (*e.g.*, NH_4^+ and NO_3^-) sharing one consumer, which inhibits the effective binding between any specific substrate and the consumer (terms $^{(1)}$ and $^{(2)}$ in Eqn. 14) and (2) multiple consumers (*e.g.*, plants, decomposing microbes, and nitrifiers)

sharing one substrate (*e.g.*, NH_4^+), which lowers the probability of effective binding between any consumer and NH_4^+ (terms $^{(3)}$, $^{(4)}$, and $^{(5)}$ in Eqn. 14).

For our reaction network (Eqn. 13 – 22), we assume that: (1) plant roots and decomposing microbes possess two types of nutrient carrier enzymes (nutrient transporters). One is for nitrogen (NH_4^+ and NO_3^-; E_N^{plant}, E_N^{mic}), and the other is for phosphorus, including different forms of phosphate (E_P^{plant}, E_P^{mic}). (2) Nutrient carrier enzyme abundance is scaled with biomass (fine root or microbial biomass). Scaling factors are 0.0000125 (for plants) and 0.05 (for decomposing microbes) (Table 2). (3) Mineral surface "effective enzyme" abundance (E_P^{surf}) is approximated by the available sorption surface area ($VMAX_P^{surf} - [SP]$). (4) Nitrifiers and denitrifiers are not explicitly simulated, therefore we assume that their biomass and associated nutrient transporter abundance are fixed (E_N^{nit}, E_N^{denit}).

For simplicity, we group the "decomposing microbes/nitrifier/denitrifier/mineral surface nutrient carrier enzyme [*E*]" and their "base reaction rate *k*" into one single variable "*VMAX*" (see Appendix B for full derivation). Furthermore, we defined "potential rates (potential immoblizaiton, nitrification, denitrification, adsorption rates)" and used them as proxies of "*VMAX*". Therefore, Eqn. 15, 16, 18, 19, 21, 22 become:

$$F_{NH4}^{immob} = F_{NH4}^{immob,pot} \cdot \frac{[NH4]}{K_M^{mic,NH4}(1+\frac{[NH4]}{K_M^{mic,NH4}}+\frac{[NO3]}{K_M^{mic,NO3}}+\frac{[E_N^{plant}]}{K_M^{plant,NH4}}+\frac{[E_N^{mic}]}{K_M^{mic,NH4}}+\frac{[E_N^{nit}]}{K_M^{nit,NH4}})} \quad (23)$$

$$F_{NH4}^{nit} = F_{NH4}^{nit,pot} \cdot \frac{[NH4]}{K_M^{nit,NH4}(1+\frac{[NH4]}{K_M^{nit,NH4}}+\frac{[E_N^{plant}]}{K_M^{plant,NH4}}+\frac{[E_N^{mic}]}{K_M^{mic,NH4}}+\frac{[E_N^{nit}]}{K_M^{nit,NH4}})} \quad (24)$$

$$F_{NO3}^{immob} = F_{NO3}^{immob,pot} \cdot \frac{[NO3]}{K_M^{mic,NO3}(1+\frac{[NH4]}{K_M^{mic,NH4}}+\frac{[NO3]}{K_M^{mic,NO3}}+\frac{[E_N^{plant}]}{K_M^{plant,NO3}}+\frac{[E_N^{mic}]}{K_M^{mic,NO3}}+\frac{[E_N^{den}]}{K_M^{den,NO3}})} \quad (25)$$

$$F_{NO3}^{den} = F_{NO3}^{den,pot} \cdot \frac{[NO3]}{K_M^{den,NO3}(1+\frac{[NO3]}{K_M^{den,NO3}}+\frac{[E_N^{plant}]}{K_M^{plant,NO3}}+\frac{[E_N^{mic}]}{K_M^{mic,NO3}}+\frac{[E_N^{den}]}{K_M^{den,NO3}})} \quad (26)$$

$$F_P^{mic} = F_P^{immob,pot} \cdot \frac{[PO_x]}{K_M^{mic,P}(1+\frac{[PO_x]}{K_M^{mic,P}}+\frac{[E_P^{plant}]}{K_M^{plant,P}}+\frac{[E_P^{mic}]}{K_M^{mic,P}}+\frac{[E_P^{surf}]}{K_M^{surf,P}})} \quad (27)$$

$$F_P^{surf} = F_P^{surf,pot} \cdot \frac{[PO_x]}{K_M^{surf,P}(1+\frac{[PO_x]}{K_M^{surf,P}}+\frac{[E_P^{plant}]}{K_M^{plant,P}}+\frac{[E_P^{mic}]}{K_M^{mic,P}}+\frac{[E_P^{surf}]}{K_M^{surf,P}})} \quad (28)$$

In this case, the potential rates are treated as maximum reaction rates (*VMAX*), because they are calculated without nutrient constraints or biotic and abiotic interactions. For example, potential P immobilization rate ($F_P^{immob,pot}$) is based on the total phosphorus demand that can perfectly maintain the soil CP stoichiometry during soil organic matter decomposition (Eqn. A9). This potential immobilization rate represents the maximum phosphorus influx that the soil could take up at that moment. The maximum adsorption rate ($F_P^{surf,pot}$) is the time derivative of the Langmuir equation (Eqn. A12), which is a theoretically maximal adsorption rate excluding all other biotic and abiotic interactions. The potential rates (*VMAX*) are updated by the model rather than calibrated, except for $VMAX_P^{surf}$. $VMAX_P^{surf}$ denotes the maximum adsorption capacity (not maximum adsorption rate), which affects the potential adsorption rate ($F_P^{surf,pot}$).

The model is run on an hourly time step, initialized with state variables and critical parameters (Table 2). Since the model is designed to be a component of the

313 Community and ACME Land Models (CLM, ALM; which are essentially currently
314 equivalent), we used CLM4.5 site-level simulations to acquire temporally-resolved: (1)
315 soil temperature factors on decomposition (r_T); (2) soil moisture factors on
316 decomposition (r_θ); (3) the anoxic fraction of soil pores (f^{anox} in Appendix Eqn. A10-
317 11); (4) annual NPP (NPP_{annual} in Appendix Eqn. A13); (5) NH_4^+ deposition (F_{NH4}^{dep}); (6)
318 NO_3^- deposition (F_{NO3}^{dep}); and (7) hydrologic discharge (Q_{dis} in Appendix Eqn. A14).
319 External inputs of mineral phosphorus are derived from Mahowald *et al.*, [2005, 2008].

320 **2.3 Model parameterization and sensitivity analysis**

321 We constrained model parameters and performed sensitivity analyses using a suite
322 of observations distinct from the observations we used subsequently to test the model
323 against the N and P manipulation experiments. Because tropical systems can be either
324 nitrogen or phosphorous limited (or both) [*Elser et al.*, 2007; *Vitousek et al.*, 2010], we
325 chose observations from a tropical forest site to constrain the N and P competition in our
326 model (Tapajos National Forest, Para, Brazil (Table 3)).

327 In the parameter estimation procedure, several data streams are assimilated into
328 the N-COM model, including measurements of soil NH_4^+ concentrations, soil free
329 phosphate concentrations, sorbed phosphate concentrations, and N_2O and CO_2 flux
330 measurements. The datasets are summarized in Table 3 and cover a wide range of N and
331 P biogeochemistry dynamics. A set of model parameters is selected for calibration (Table
332 4), which comprise nutrient competition kinetics parameters (k and K_M) as well as the fast
333 soil carbon turnover time ($TURN_{SOM}$). Because we had only a short-term CO_2 respiration
334 flux record, we were unable to calibrate the longer turnover time parameters. However,
335 since we test the calibrated model against short-term fertilization responses, this omission

will not affect our evaluation. Longer records from eddy covariance flux towers and ^{14}C soil measurements are required to constrain the longer turnover time pool values.

We employed the Markov Chain Monte Carlo (MCMC) approach [*Ricciuto et al.*, 2008] to assimilate the observations into N-COM. MCMC directly draws samples from a pre-defined parameter space and tries to minimize a pre-defined cost function:

$$J = (M(\theta) - D)^T R^{-1} (M(\theta) - D) \quad (29)$$

where $\boldsymbol{M(\theta)}$ and $\boldsymbol{D}$ are vectors of model outputs and observations including time series of different simulated variables (*e.g.*, soil CO_2 and N_2O effluxes and soil concentrations of NH_4^+, free PO_x, and sorbed PO_x); $\boldsymbol{\theta}$ is a vector of model parameters ($\boldsymbol{\theta_i}$); and $\boldsymbol{i}$ from 1 to 20 represents the parameters that are calibrated (Table 4). R^{-1} is the inverse of data error covariance matrix. We assumed that diagonal elements are 40% of observed values and off-diagonal elements are zeros. We further assumed that the prior parameter follows a lognormal distribution. μ and σ were 0.91 and 0.95 of their initial values, respectively (Table 4). We then ran MCMC to sample 50,000 parameter pairs (Fig. A1). The second half of the samples was fit to a Gaussian distribution. We also employed the Gelman-Rubin criterion to quantitatively show whether or not the MCMC chain converged. The calibrated model parameters are reported in term of means and standard deviations. Uncertainty Reduction (*UR*) is calculated based on (1) variance (Eqn. 30a) and (2) 25% and 75% quantile (Eqn. 30b):

$$UR_\sigma = (1 - \frac{\sigma_{posterior}}{\sigma_{prior}}) \cdot 100\% \quad (30a)$$

$$UR_Q = (1 - \frac{Q^{75}_{posterior} - Q^{25}_{posterior}}{Q^{75}_{prior} - Q^{25}_{prior}}) \cdot 100\% \quad (30b)$$

where σ_{prior} is prior parameter uncertainty, which is 95% of the parameter initial value. $\sigma_{posterior}$ is calibrated parameter uncertainty, which is calculated by fitting the calibrated model parameters to a Gaussian distribution. Q^{75} and Q^{25} are 75% and 25% percentage quantile of each parameter. Uncertainty Reduction is a useful metric [*Zhu and Zhuang*, 2014], because it quantitatively reveals the reduction in the range of a particular parameter after calibration with MCMC. It does not, however, indicate that the parameter itself is more consistent with observed values of the parameter. A large value of *UR* implies a more robust model.

In addition, we conducted a sensitivity study to identify the dominant controlling factors regulating nutrient competition in N-COM. Three scenarios were considered: (1) baseline climate and soil conditions; (2) elevated soil temperature (by 5 °C); and (3) elevated soil moisture (by 50%). SOBOL sampling [*Pappas et al.*, 2013], a global sensitivity technique, is employed to calculate the sensitivities of output variables with respect to various inputs:

$$S_i = \frac{VAR_{p_i}(E_{p_{\sim i}}(Y \mid p_i))}{VAR(Y)} \tag{31}$$

where S_i is the first order sensitivity index of the i^{th} parameter and ranges from 0 to 1. By comparing the values of S_i, we were able to evaluate which processes affect the pattern of nutrient competition. Y represents the model outputs of plant NH_4^+, NO_3^-, or PO_x uptake; p_i is the target parameter; $p_{\sim i}$ denotes all parameters that are associated with nutrient competition except the target parameter; and *VAR(.)* and *E(.)* represent variance and mean, respectively.

2.4 Model application

After calibration, we applied the N-COM model to several tropical forest nutrient fertilization studies not included in the calibration dataset, where isotopically labeled nitrogen or phosphorous fertilizer was injected into the soil. The fertilization experiments measured the fate of added nutrients; for example, identifying the fraction of added N or P that goes into the plant, is immobilized by microbes, or is stabilized by mineral surfaces. These measurements offer an effective baseline to test whether the N-COM model captures short-term nutrient competition.

Because we have focused in this paper on applications in tropical forests, we choose three tropical forest fertilization experiments with (1) PO_4^{3-}; (2) NH_4^+; and (3) NO_3^- additions (Table 5). The PO_4^{3-} fertilization experiment [*Olander and Vitousek*, 2005] was conducted in three Hawaiian tropical forests along a soil chronosequence (300, 20000, and 4100000 year old soils) that were fertilized with 10 μg g^{-1} $^{32}PO_4^{3-}$, respectively, and microbial demand versus soil sorption was measured. We did not evaluate the role of plants in phosphorus competition for the Hawaii sites, since plant phosphorus uptake was not measured in those field studies. Our model discriminates the Hawaii sites along the chronosequence by setting distinct initial pool sizes (derived from [*Olander and Vitousek*, 2004; *Olander and Vitousek*, 2005]) of soil organic carbon, nitrogen and phosphorus, and soil parent material phosphorus.

We also used measurements from NH_4^+ and NO_3^- fertilization studies located at the Luquillo tropical forest in Puerto Rico [*Templer et al.*, 2008]. In that study, 4.6 μg g^{-1} $^{15}NH_4^+$ was added into the highly weathered tropical forest soil and the consumption of $^{15}NH_4^+$ by plant roots, decomposing microbes, and nitrifiers were measured. In the same study, 0.92 μg g^{-1} $^{15}NO_3^-$ was added to the soil and the plant uptake and microbial

immobilization was measured. The measurements were made 24 or 48 hours after the fertilizers were added.

For the model scenarios, we (1) spun up the N-COM model for 100 years; (2) perturbed the soil nutrient pool by the same amount as the fertilization; (3) ran the model for 24 or 48 hours and calculated how much of the added nutrients were absorbed by plants, microbes, or mineral surfaces; and (4) compared our model simulations with the observed data to assess model predictability. The 100-year spin up simulation aimed at eliminating the effects of imposed initial inorganic pool sizes on fertilization experiments, rather than accumulating soil organic matter in the system, since we initialized the soil organic carbon pools from CLM4.5 steady state predictions.

3. Results and discussion

3.1 Calibrated model parameters

Our best estimates (second half of the MCMC chain) of the selected model parameters based on the observations at the Tapajos National Forest, Para, Brazil are shown in Figure 2. We found that calibrated parameter samples were not heavily tailed and they generally follow Gaussian distributions (Figure A3). In order to quantitatively compare the calibrated parameter distributions with prior distributions, we fit parameter samples to a Gaussian distribution and estimated its means and standard deviations (Table 4).

Even though the parameter mean was improved, the uncertainty may still be relatively large. In other words, a prognostic prediction based on these calibrated parameters could be relatively uncertain [*Scholze et al.*, 2007], due to large uncertainty

associated with the calibrated parameters. Therefore, we calculated the variance-based Uncertainty Reduction (UR_{σ}) (Eqn. 30a) to evaluate model improvement in terms of parameter uncertainty. We found that parameters' uncertainties were reduced by 13%~98%. This calculation might either overestimate or underestimate the UR_{σ}, due to the fact that the calibrated parameters did not strictly follow Gaussian distributions. But the actual UR_{σ} should not be far from our estimates, because these samples were not widely spread across the potential parameter space (Figure 2). The least constrained parameter was k_{NO3}^{plant} (reaction rate of plant nitrogen carrier enzyme with NO_3^- substrate). Two other NO_3^- dynamics related parameters were also not well constrained: UR_{σ} of $K_M^{mic,NO3}$ (half-saturation constant for decomposing microbe NO_3^- immobilization) and $K_M^{den,NO3}$ (half-saturation constant for denitrifier NO_3^- consumption) were only 63% and 68%, respectively. Compared with NH_4^+ or PO_x competition related parameters, we concluded that parameters associated with NO_3^- competition were the least constrained in the model. This result was primarily due to the lack of NO_3^- pool size data, and secondarily due to the fact that NO_3^- was not the major nitrogen source for plant or decomposing microbes. We also provide quantile-based Uncertainty Reduction for reference (Table 4). The above-mentioned conclusions still hold with quantile-based UR_Q, although the quantile-based UR_Q is generally higher than variance-based UR_{σ}. One parameter was calibrated to be at the upper boundary of its prior ranges (k_P^{plant}), implying that this tropical plant is highly efficient in phosphorus uptake. Although we do not have direct kinetic parameter observations for the specific tropical species involved in our study, an inferred high phosphorus uptake efficiency is reasonable for tropical species

that have adapted to these phosphorus deficient environments [*Begum and Islam*, 2005; *FÖHse et al.*, 1988].

Convergence of model parameters is reported with the Gelman-Rubin criterion (univariate potential scale reduction factor) (Table 4 and Figure A2). Using this criterion, seven (out of twenty) parameters are found to converge (Gelman-Rubin <= 1.1). The lack of convergence (in addition, 20-dimensional multivariate potential scale reduction factor is 12.04) of the remaining parameters is partly due to data paucity. In particular, starting from different initial values, MCMC calibrations may result in different models that give rise to similar model-data misfit (i.e., "equifinality" [*Tang and Zhuang*, 2008]). In this regard, high frequency measurements may improve model calibration (see more discussion in **section 3.3**). The non-convergence of model parameters implies an imperfect model. Therefore, for large-scale model application, more work on data collection, parameter tuning, and uncertainty analysis is needed. However, even with these caveats, the model predictability is reasonably good when applied to the tropical forest fertilization experiments described in Section 3.4.

Berkeley Lab 12/16/15 11:10 PM
Comment [1]: modified

We re-organize the right hand sides of Eqns. 14 – 22 to be the product of potential nutrient uptake rate and an ECA limitation term; for example for plant NH_4^+ uptake:

$$F_{NH4}^{plant} = k_{NH4}^{plant} \cdot ECA_{NH4}^{plant} \tag{32}$$

$$ECA_{NH4}^{plant} = \frac{[NH4]\cdot[E_N^{plant}]}{K_M^{plant,NH4}\left(1+\frac{[NH4]}{K_M^{plant,NH4}}+\frac{[NO3]}{K_M^{plant,NO3}}+\frac{[E_N^{plant}]}{K_M^{plant,NH4}}+\frac{[E_N^{mic}]}{K_M^{mic,NH4}}+\frac{[E_N^{nit}]}{K_M^{nit,NH4}}\right)} \tag{33}$$

Other "consumer-substrate reactions" have similar forms. Under a nutrient abundant situation (*e.g.*, fertilized agriculture ecosystem), the relative competitiveness of each consumer (*ECA*) is dominated by its specific enzyme abundance ([*E*]). Under such

conditions, substrate affinity is no longer a controlling factor. In contrast, under nutrient limited conditions (*e.g.*, many natural ecosystems), ECA is dominated by the specific enzyme abundance as well as the substrate affinity ($[E]/K_M$). Therefore, consumers could either enable an alternative high affinity nutrient transporter system (low K_M) or exude more enzyme to enhance competitiveness. For example, at the whole-soil scale it has been shown that root spatial occupation (C_{froot}) determines a plant's competitiveness when low soil nutrient diffusivity is limiting nutrient supply [*Raynaud and Leadley*, 2004]. Consistently, our results highlighted the dominant role of nutrient carrier enzyme abundance (E proportional to C_{froot}) in controlling competition. If we further assumed that plants, decomposing microbes, and nitrifiers enzyme abundances were approximately equal, we will have that the relative their competitiveness in acquiring NH_4^+ was about 4:10:9 ($1/K_M^{plant,NH4} : 1/K_M^{mic,NH4} : 1/K_M^{nit,NH4}$). However, such results could not be easily generalized to other ecosystems, because they heavily relied on the traits (affinity) of specific competitors. For a different ecosystem, those traits would be drastically different due to the change of, *e.g.*, plant species composition and microbial community structure. Even for the same ecosystem, those traits could be highly heterogeneous. For example, the community structure of decomposing microbes could be different in rhizosphere and bulk soil (with different K_M). However, in this work we assumed a well-mixed environment (one soil column), in order to be consistent with large-scale ecosystem models. Although beyond the scope of the current study, the consequences of ignoring the rhizosphere versus bulk soil heterogeneity warrants further investigation. Large-scale models aim to quantify ecosystem level dynamics, although they are usually driven by parameters inferred from *in situ* field observations. In the

492 absence of a model that explicitly represents this spatial heterogeneity, it is difficult to
493 quantify the impacts of using inferred rhizosphere decomposer affinities on model
494 predictions of the whole soil [*Schimel et al.*, 1989]. Furthermore, the assumption of well-
495 mixed environment in large-scale model is an inevitable flaw, because of large
496 computational demands and a lack of scale-aware parameters and model structures for
497 large-scale models to run fine scale simulations.

498 Although in this study ECA was applied to a large-scale model, the competition
499 framework is readily applicable to fine scale models that consider soil heterogeneity. In
500 fine-scale models, bulk soil nutrient competition can occur only among different
501 microbes because they are ubiquitous in the soil (*e.g.*, nitrifier versus microbial
502 decomposer), while rhizosphere nutrient competition occurs among plants and microbes
503 (*e.g.*, nitrifier versus microbial decomposer versus roots). This distinction implies that the
504 competitiveness parameters we infer here for N-COM, which does not currently
505 explicitly represent bulk versus rhizosphere processes, subsume the range of fine scale
506 processes controlling nutrient uptake. More research is required to link these different
507 model spatial scales, theory, and parameterizations.

508 Our modeling framework highlights the important concept that "competitiveness"
509 is a dynamic property of the competition network, and more importantly that it is linked
510 to competitor functional traits (affinity and nutrient carrier enzyme abundance). This
511 concept is in contrast to the prevailing assumption underlying all major large-scale
512 ecosystem models, which either assume "relative demand competitiveness for different
513 nutrient consumers" [*Thornton et al.*, 2007] or "soil microbes outcompete plants"
514 [*McGuire et al.*, 1992; *Parton et al.*, 1988]. Imposing such pre-defined orders of

competitiveness neglects the diversity of nutrient competitors (plants and microbes) and their differences in nutrient uptake capacity expressed by relevant functional traits. Our model framework offers a theoretically consistent approach to account for the diversity of nutrient competition in different competitor networks.

3.2 Model sensitivity analysis

Through sensitivity analysis, we separately investigated the factors controlling plant NH_4^+, NO_3^-, and PO_x competition (Figure 3). Each sensitivity analysis consisted of three scenarios: (1) normal conditions (control); (2) elevated soil temperature ($+T_s$); and (3) elevated soil moisture ($+\theta$). The sensitivity analysis indicates that the model is highly sensitive to kinetics parameters (*e.g.*, K_M). Furthermore, the model is consistently sensitive to the same parameters across all temperature and moisture conditions. The environment affects the nutrient competition primarily through altering the nutrient abundance. Enhanced soil temperature and soil moisture accelerated soil organic carbon turnover, thereby releasing more inorganic nutrient into the soil (gross mineralization). However, the impacts on plant nutrient uptake are limited (Figure 3) because the enhanced soil organic matter decay also requires higher immobilization fluxes to sustain the soil organic matter CNP stoichiometry. The enhancement of net mineralization would be limited, and therefore would not change soil nutrient status dramatically.

3.3 Model performance

The prior and calibrated models were compared against observational datasets of pool sizes of soil free phosphate, sorbed phosphate, and NH_4^+, CO_2 efflux, and N_2O efflux (Figure 4). We note that although we attempted to acquire as many datasets that contained these five observations as possible, more observations in tropical ecosystems

would clearly improve the parameter estimates. For example, in the experiment we analyzed, only three measurements of soil free phosphate were made during 1999. Many detailed dynamics are therefore missing and could impact our parameter estimates. The prior model predicted an increasing trend of soil free PO_x, which resulted from underestimates of plant P uptake (by underestimating of k_P^{plant}) and soil microbial P immobilization (by overestimating $K_M^{mic,P}$). The calibrated model captured the seasonal dynamics of soil free PO_x reasonably well: increases during the wet season and gradual decreasing during the dry season (August to November). The prior model also largely underestimated the seasonal variability of nitrogen dynamics and underestimated the NH_4^+ pool size due to overestimation of plant NH_4^+ uptake (k_{NH4}^{plant}). In addition, it also underestimated the denitrification N_2O emissions, because of an underestimation of NH_4^+ to NO_3^- transformation rate (k_{nit}). Consequently, there was not enough NO_3^- substrate to react with denitrifiers and release N_2O. The calibrated model, however, accurately reproduced the seasonal dynamics of both NH_4^+ pool sizes and soil N_2O emissions. There were small differences between the prior and calibrated model predictions of soil CO_2 emissions. The CO_2 and N_2O effluxes were more frequently observed at Tapajos National Forest during 1999 to 2001, compared with phosphorus data. Most of the measurements were collected during the wet season. Therefore the modeled CO_2 and N_2O emissions were largely improved by assimilating these datasets.

The model performance implies that after assimilating multiple datasets, our model predictions were improved over the prior model. However, it is clear that more observations of the metrics applied in our MCMC approach would benefit the model calibration. Unfortunately, because of our focus on tropical sites, we were unable to

561 acquire more datasets that had the full suite of measurements required. Datasets of soil
562 nutrient pool sizes (*e.g.*, NO_3^-) and higher frequency sampling of those sparse
563 measurements (*e.g.*, POx) would significantly benefit the model uncertainty reduction.

564 **3.4 Model testing against nitrogen and phosphorus fertilization studies**

565 To test the calibrated N-COM model, we conducted short-term numerical
566 competition experiments (24-hour or 48-hour simulations) by manually imposing an
567 input flux into nutrient pools equivalent to the N and P fertilization experiments
568 described above and in Table 5. The simulated results were compared with observations
569 from the field manipulations.

570 In the P addition experiments across the Hawaiian chronosequence, the
571 partitioning of phosphate between microbes and mineral surfaces was well represented by
572 the N-COM model in the intermediate (20K yr) and old (4.1M yr) sites (Figures 5b and
573 5c), with no significant differences between model predictions and observations. In the
574 youngest Hawaiian site (300 yr; Figure 5a), the relative partitioning was correctly
575 simulated, but the predicted PO_4^{3-} magnitudes were lower than observations. Our
576 simulations indicated that at the young soil site the added P exceeded microbial demand,
577 resulting in lower predicted microbial P uptake than observed. This discrepancy reflected
578 a possible deficiency of first-order SOC decay models (as we used here), which implicitly
579 treat microbes as a part of soil organic matter. Since microbial nutrient immobilization is
580 strictly regulated by the SOC turnover rate in this type of model, external nutrient inputs
581 will no longer affect microbial nutrient uptake if the inputs exceed potential microbial
582 demand. We therefore believe that explicit Microbe-Enzyme models might be able to
583 better explain the strong microbe PO_4^{3-} uptake signal observed at the young Hawaii

584 fertilization experiment site. Microbial models explicitly simulate the dynamics of
585 microbial biomass, which might be able to capture the expected rapid growth of
586 microbial communities under conditions of improved substrate quality [*Kaspari et al.*,
587 2008; *Wieder et al.*, 2009].

588 In the Puerto Rican Luquillo forest nitrogen addition experiments, partitioning of
589 added ammonium between plants and heterotrophic bacteria was well captured by the N-
590 COM model, with no significant differences between model predictions and observations
591 (Figure 5d). However, the model underestimated nitrifier NH_4^+ uptake. NO_3^- competition
592 in this site was also relatively accurately predicted (Figure 5e), although the
593 measurements did not include denitrification. Model estimates of plant NO_3^- uptake and
594 microbial NO_3^- immobilization were consistent with the observed ranges, but we
595 highlight the large observational uncertainties, particularly for microbial NO_3^- uptake.

596 In the pseudo-first-order decomposition model we applied here to demonstrate the
597 ECA competition methodology, the soil organic matter C:N:P ratio also limited microbial
598 N and P uptake. For this type of decomposition model, stoichiometric differences
599 between soil organic matter and microbes are not dynamically simulated. Such a
600 simplification of soil and microbial stoichiometry favors large spatial scale model
601 structures over long temporal periods, but hampers prediction of microbial short-term
602 responses to N and P fertilization. For example, the observed difference between
603 microbial and soil C:P ratios can be as large as 6-fold [*Mooshammer et al.*, 2014; *Xu et*
604 *al.*, 2013]. Were that the case in the observations we applied, the potential soil P demand
605 calculated based on a fixed soil organic matter C:P ratio could be only 17% of that based
606 on microbial C:P ratio.

3.5 Implications of ECA competition treatment

Terrestrial ecosystem growth and function are continuously altered by climate (*e.g.*, warming, drought; [*Chaves et al.*, 2003; *Springate and Kover*, 2014]), external nutrient inputs (*e.g.*, N deposition; [*Matson et al.*, 2002; *Matson et al.*, 1999]), and atmospheric composition (*e.g.*, CO_2 concentration; [*Norby et al.*, 2010; *Oren et al.*, 2001; *Reich et al.*, 2006]). Improved understanding of the underlying mechanisms regulating ecosystem responses to environmental changes has been obtained through *in situ* level to large-scale and long-term manipulation experiments. For example, decade-long Free-Air Carbon Dioxide Enrichment (FACE) experiments have revealed that nitrogen limitation diminished the CO_2 fertilization effect of forests [*Norby et al.*, 2010] and grasslands [*Reich and Hobbie*, 2013] ecosystems. However, fewer efforts have been made towards incorporating the observed process-level knowledge into Earth System Models (ESMs). Therefore, a major uncertainty that has limited the predictability of ESMs has been the incomplete representation of soil nutrient dynamics [*Zaehle et al.*, 2014]. Even though new soil nutrient cycle paradigms were proposed during recent decades [*Korsaeth et al.*, 2001; *Schimel and Bennett*, 2004], they were restricted to either conceptual models or only applied to explain laboratory experiments.

Many large-scale terrestrial biogeochemistry models (*e.g.*, O-CN, CASA, TEM) have adopted the classical paradigm that microbes decompose soil organic matter and release NH_4^+ as a "waste" product [*Waksman*, 1931]. The rate of this process is defined as "net N mineralization", and is adopted as a "measure" of plant available inorganic N [*Schimel and Bennett*, 2004]. This classical paradigm overlooked the fact that "net N mineralization" actually comprised two individual processes - gross N mineralization and

630 microbial N immobilization. Implicitly, the classical paradigm assumes that the microbes
631 have priority to assimilate as much of the available nutrient pool as possible. Soil
632 nutrients were only available for plant uptake if there were not enough free energy
633 materials (*e.g.*, dissolved soil organic carbon) to support microbial metabolism. As a
634 result, soil microbes were considered "victors" in the short-term nutrient competition.
635 Some other large-scale terrestrial biogeochemistry models (*e.g.*, CLM4CN), simplify the
636 concept of nutrient competition differently. They calculate the plant N uptake and soil N
637 immobilization separately; and then down-regulate the two fluxes according to the soil
638 mineral N availability. As a result, plant and soil microbe competitiveness for nutrients is
639 determined by their relative demand.

640 Climate-scale land models have over-simplified or ignored competition between
641 plants, microbes, and abiotic mechanisms. In reality, under high nutrient stress
642 conditions, plants can exude nutrient carrier enzymes or facilitate mycorrhizal fungi
643 associations to enhance competitiveness for nutrient acquisition [*Drake et al.*, 2011;
644 *Hobbie and Hobbie*, 2006; *Treseder and Vitousek*, 2001]. In addition, plants can adjust C
645 allocation to construct more fine roots, which scavenge nutrients over larger soil volumes
646 [*Iversen et al.*, 2011; *Jackson et al.*, 2009; *Norby et al.*, 2004]. Soil spatial heterogeneity
647 might also contribute to the success of plant nutrient competition [*Korsaeth et al.*, 2001].
648 Therefore, most ecosystem biogeochemistry models with traditional treatments of
649 nutrient competition likely underestimate plant nutrient uptake.

650 Nutrient competition should be treated as a complex consumer-substrate reaction
651 network: multiple 'consumers', including plant roots, soil heterotrophic microbes,
652 nitrifiers, denitrifiers, and mineral surfaces, each competing for substrates of organic and

653 inorganic nitrogen and phosphorus as nutrient supply. In such a model structure, the
654 success of any consumer in substrate acquisition is affected by its consumer-substrate
655 affinity [*Nedwell*, 1999]. Such competitive interactions have been successfully applied to
656 microbe-microbe and plant-microbe substrate competition modeling [*Bonachela et al.*,
657 2011; *Lambers et al.*, 2009; *Maggi et al.*, 2008; *Maggi and Riley*, 2009; *Moorhead and*
658 *Sinsabaugh*, 2006; *Reynolds and Pacala*, 1993] for many years.
659 Here, we applied the consumer-substrate network in a broader context of plant,
660 microorganism, and abiotic mineral interactions. We analyzed the consumer-substrate
661 network using a first-order accurate equilibrium chemistry approximation (ECA) [*Tang*
662 *and Riley*, 2013; *Zhu and Riley*, 2015]. Our sensitivity analysis confirmed that the
663 consumer-substrate affinity and nutrient carrier enzyme abundance were the most
664 important factors regulating relatively short-term competitive interactions. The ECA
665 competition treatment represents ecosystem responses to environmental changes and has
666 the potential to be linked to a microbe-explicit land biogeochemistry model. The
667 approach allows competition between plants, microbes, and mineral surfaces to be
668 prognostically determined based on nutrient status and capabilities of each consumer.
669
670 **4. Conclusions**
671 In this study, we developed a soil biogeochemistry model (N-COM) that resolves
672 the dynamics of soil nitrogen and phosphorus, plant uptake of nutrients, microbial uptake,
673 and abiotic interactions. We focused on the implementation, parameterization, and testing
674 of the nutrient competition scheme that we plan to incorporate into the ESM land models
675 CLM and ALM. We described the multiple-consumer and multiple-nutrient competition

676 network with the Equilibrium Chemical Approximation (ECA) [*Tang and Riley*, 2013]
677 considering two inhibitive effects: (1) multiple substrates (*e.g.*, NH_4^+ and NO_3^-) sharing
678 one consumer inhibits the effective binding between any specific substrate and the
679 consumer and (2) multiple consumers (*e.g.*, plants, decomposing microbes, nitrifers)
680 sharing one substrate (*e.g.*, NH_4^+) lowers the probability of effective binding between any
681 consumer and that substrate. We calibrated the model at a tropical forest site with highly
682 weathered soil (Tapajos National Forest, Para, Brazil), using multiple observational
683 datasets with the Markov Chain Monte Carlo (MCMC) approach. The calibrated model
684 compared to multiple categories of observational data was substantially improved over
685 the prior model (Figure 4). The seasonal dynamics of soil carbon, nitrogen, and
686 phosphorus were moderately well captured. However, our results would likely be more
687 robust if more temporally resolved observations of carbon, nitrogen, and phosphorous
688 were available. Although the calibrated model is the best one we can derive based on
689 limited data, several model parameters were not well converged. We therefore conclude
690 that more work on data collection, parameter tuning, and uncertainty analysis is needed.
691 To test the resulting model using the calibrated parameters, we applied N-COM to
692 two other tropical forests (Hawaii tropical forest and Luquillo tropical forest) not used in
693 the calibration process and conducted nutrient perturbation studies consistent with
694 fertilization experiments at these sites. The results showed that N-COM simulated the
695 nitrogen and phosphorus competition well for the majority of the observational metrics.
696 However, the model underestimated NH_4^+ uptake by nitrifiers, probably due to the
697 loosely constrained nitrification parameters that were the result of NO_3^- pool size data
698 paucity during calibration at the Brazil site (Table 4). Datasets of soil nutrient pool sizes

699 and CO_2 and N_2O effluxes with high frequency sampling would significantly benefit the
700 model uncertainty reduction.
701 To date, many terrestrial ecosystem biogeochemistry models assume microbes
702 outcompete plants and immobilize nutrients first [*Y P Wang et al.*, 2007; *Zaehle and*
703 *Friend*, 2010; *Zhu and Zhuang*, 2013], although CLM currently assumes constant and
704 relative demand competitiveness of plants and microbes. Few models, to our knowledge,
705 consider the role of abiotic interactions in the competitive interactions. In the case of
706 microbes outcompeting plants, the plant is only able to utilize the nutrients that exceed
707 microbial demands during that time step. The leftover nutrients are defined as net
708 mineralization, which is a widely adopted concept in soil biogeochemistry modeling
709 [*Schimel and Bennett*, 2004]. These models oversimplify plant-microbe interactions by
710 imposing dubious assumptions (*e.g.*, microbes always win against plants). We showed
711 that (in section 3.1) "competitiveness" is a dynamic rather than fixed property of the
712 competition network, and more importantly, it should be linked to competitor functional
713 traits (affinity and nutrient carrier enzyme abundance).
714 This study is an important step towards implementing more realistic nutrient
715 competition schemes in complex climate-scale land models. Traditional ESMs generally
716 lack realistic soil nutrient competition, which likely biases the estimates of terrestrial
717 ecosystem carbon productivity and biosphere-climate feedbacks. This study showed the
718 effectiveness of ECA kinetics in representing soil multiple-consumer and multiple-
719 nutrient competition networks. Offline calibration and independent site-level testing is
720 critically important to ensuring the newly incorporated model will perform reasonably
721 when integrated in a complex ESM. To this end, we provide a universal calibration

approach using MCMC, which could in the future be used to further constrain N-COM across plant functional types, climate, and soil types.

Acknowledgements: This research was supported by the Director, Office of Science, Office of Biological and Environmental Research of the US Department of Energy under Contract No. DE-AC02-05CH11231 as part of the Regional and Global Climate Modeling (RGCM) and ACME programs.

729 **Figure 1.** Model structure. Boxes represent pools, solid arrows represent aqueous fluxes,
730 and dashed arrows represent gaseous pathways out or into the system. Three essential
731 chemical elements (Carbon (C), Nitrogen (N) and Phosphorus (P)) are simulated in N-
732 COM (blue, red, and green represent C, N, and P pools and processes, respectively).
733

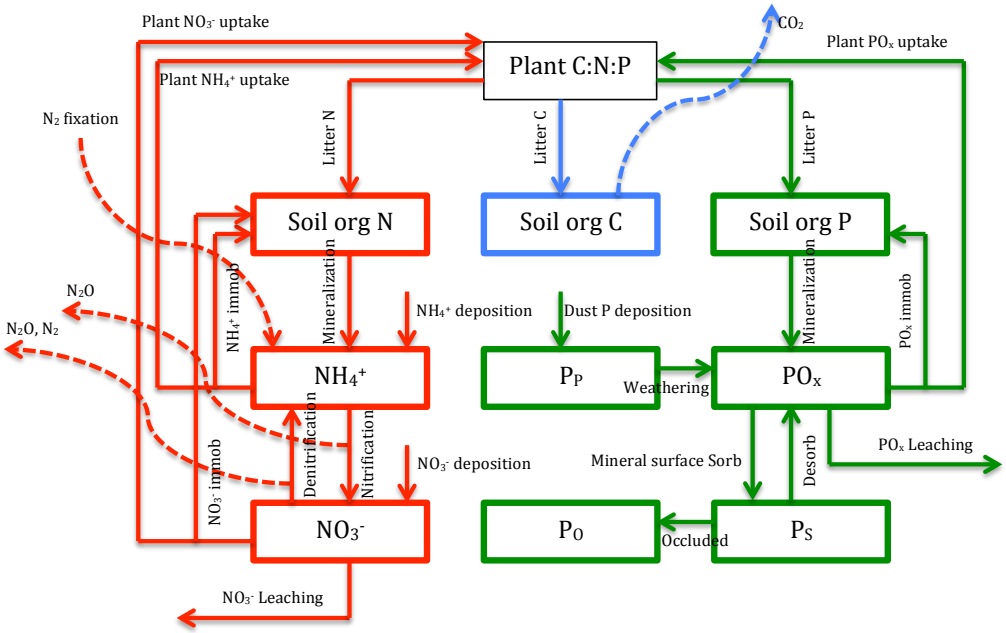

Figure 2. Distribution of prior and calibrated model parameters.

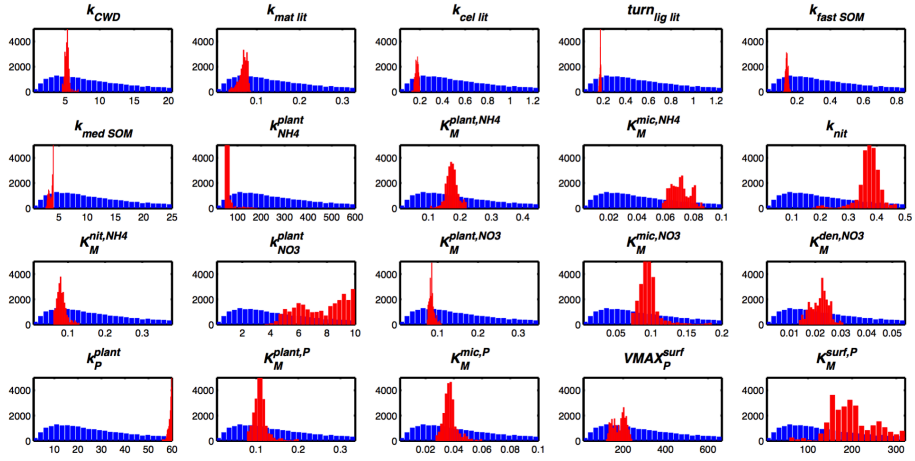

Figure 3. Model sensitivity analysis with SOBOL sampling. For each metric, three scenarios are shown: baseline (Control), elevated soil temperature by 5 °C ($+T_s$), and elevated soil moisture by 50% ($+\theta$), respectively. The length of bar (plot in polar coordinate) is the sensitivity (unit-less) of model output with respect to model input variables. Our results showed that the plant nutrient uptake was mostly regulated by internal consumer-substrate uptake kinetics rather than the external environmental conditions (*e.g.*, T_s, θ).

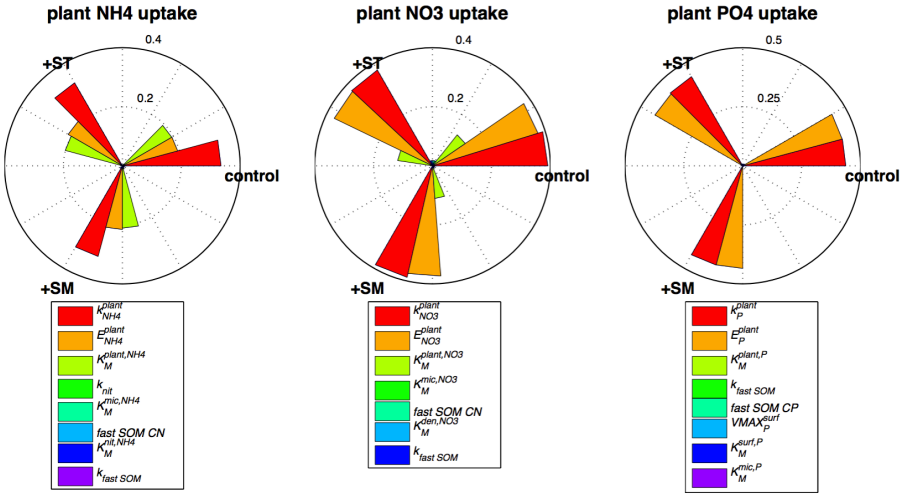

Figure 4. Model performance at Tapajos National Forest, Para, Brazil. Overall, the calibrated model (blue line) improved predictions over the prior model (grey line) when compared to observations. Green areas indicate the calibrated model uncertainties.

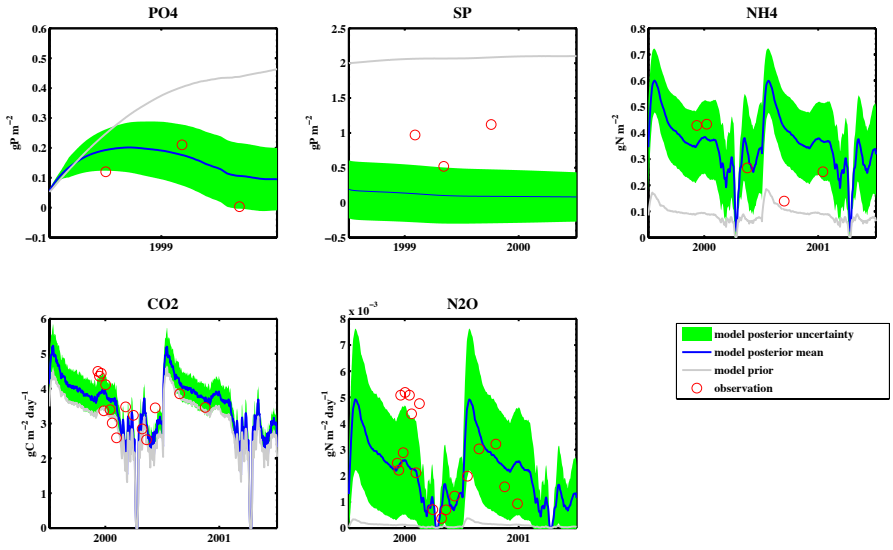

Figure 5. Model perturbation experiments compared with nitrogen and phosphorus fertilization field experimental data. The blue dots show the difference between control and perturbed simulations, which mean how much newly added nutrient each consumer takes up. The red circles are recovered isotopically labeled nutrient within each consumer. Since plants phosphorus uptake was not measured at Hawaii sites, we didn't include the plants in the perturbation study.

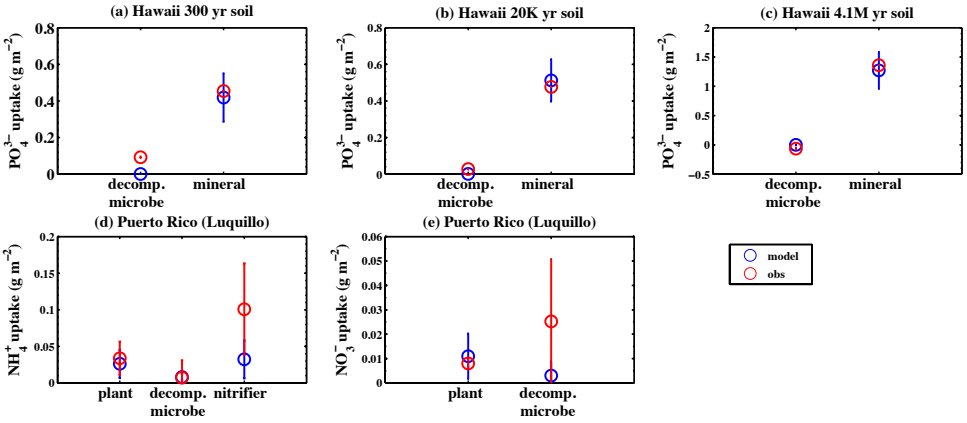

757 **Table 1.** A summary of the modeled consumer-resource competition network.

Resources	**Consumers**		
NH_4^+	Plant	Decomposing Microbe	Nitrifier
NO_3^-	Plant	Decomposing Microbe	Denitrifier
PO_x	Plant	Decomposing Microbe	Mineral surface

758

Table 2. Model parameters and baseline values.

C associated				
g_i	Percentage of carbon remains in the soil after decomposition of i^{th} SOM	-	[1.0; 0.45; 0.5; 0.5; 0.83; 0.45; 0.45]	[*Koven et al.*, 2013]
f_{ij}	fraction of SOM leave from i^{th} pool and enter into j^{th} pool	-	[0, 0, 0.76, 0.24, 0, 0, 0; 0, 0, 0, 0, 1, 0, 0; 0, 0, 0, 0, 1, 0, 0; 0, 0, 0, 0, 0, 1, 0; 0, 0, 0, 0, 0, 0.995, 0.005; 0, 0, 0, 0, 0.93, 0, 0.07; 0, 0, 0, 0, 1, 0, 0]	[*Koven et al.*, 2013]
CN	Soil organic matter CN ratio	-	[13,16,7.9]	[*Parton et al.*, 1988]
CP	Soil organic matter CP ratio	-	[110,320,114]	[*Parton et al.*, 1988]
$TURN_{SOM}$	Soil organic matter turn over [CWD, metabolic lit, cellulose lit, lignin lit, fast SOM, medium SOM, slow SOM]	year	[4.1, 0.066, 0.25, 0.25, 0.17, 5, 270]	[*Koven et al.*, 2013]
N associated				
k_{NH4}^{plant}	Reaction rate of plant NH_4^+ carrier enzyme	day^{-1}	120 (a)	[*Jackson et al.*, 1997; *Min et al.*, 2000]
$K_M^{plant,NH4}$	Half-saturation constant for plant NH_4^+ uptake	$g\ m^{-2}$	0.09	[*Kuzyakov and Xu*, 2013]
$K_M^{mic,NH4}$	Half-saturation constant for decomposing microbe NH_4^+ immobilization	$g\ m^{-2}$	0.02	[*Kuzyakov and Xu*, 2013]
k_{nit}	Maximum fraction of NH_4^+ pool that could be utilized by nitrifiers	day^{-1}	10%	[*Parton et al.*, 2001]
$K_M^{nit,NH4}$	Half-saturation constant for nitrifier NH_4^+ consumption	$g\ m^{-2}$	0.076	[*Drtil et al.*, 1993]
k_{NO3}^{plant}	Reaction rate of plant NO_3^- carrier enzyme	day^{-1}	2 (a)	[*Jackson et al.*, 1997; *Min et al.*, 2000]
$K_M^{plant,NO3}$	Half-saturation constant for plant NO_3^- uptake	$g\ m^{-2}$	0.07	[*Kuzyakov and Xu*, 2013]
$K_M^{mic,NO3}$	Half-saturation constant for decomposing microbe NO_3^- immobilization	$g\ m^{-2}$	0.04	[*Kuzyakov and Xu*, 2013]
$K_M^{den,NO3}$	Half-saturation constant for denitrifier NO_3^- consumption	$g\ m^{-2}$	0.011	[*Murray et al.*, 1989]
$[E_N^{plant}]$	Plant nitrogen carrier enzyme abundance for nitrogen uptake	$g\ m^{-2}$	$C_{froot} \cdot 0.0000125$ (a)	[*Tang and Riley*, 2013; *Trumbore et al.*, 2006]
$[E_N^{mic}]$	Decomposing microbes nitrogen carrier enzyme abundance for nitrogen immobilization	$g\ m^{-2}$	$\frac{F_N^{immob,pot}}{1000}$ (b)	[*Tang and Riley*, 2013]
$[E_N^{nit}]$	Nitrifier nitrogen carrier enzyme abundance for NH_4^+ assimilation	$g\ m^{-2}$	$1.2E^{-3}$	[*Raynaud et al.*, 2006]

$[E_N^{den}]$	Denitrifier nitrogen carrier enzyme abundance for NO_3^- assimilation	g m^{-2}	1.2E^{-3}	[*Raynaud et al.*, 2006]
f^{N2O}	Fraction of nitrification flux lost as N_2O	-	6E^{-4}	[*Li et al.*, 2000]
P associated				
$k_{weather}$	Parent material P weathering rate	g P m^{-2} year^{-1}	0.004	[*Y P Wang et al.*, 2010]
k_{occl}	P occlude rate	month^{-1}	1.0E^{-6}	[*Yang et al.*, 2014]
k_P^{plant}	Reaction rate of plant PO_x carrier enzyme	day^{-1}	12 (a)	[*Colpaert et al.*, 1999]
$K_M^{plant,P}$	Half-saturation constant for plant PO_x uptake	g m^{-2}	0.067	[*Cogliatti and Clarkson*, 1983]
$K_M^{mic,P}$	Half-saturation constant for decomposing microbe PO_x immobilization	g m^{-2}	0.02	[*Chen*, 1974]
$VMAX_P^{surf}$	Maximum mineral surface PO_x adsorption	g m^{-2}	133	[*Y P Wang et al.*, 2010]
$K_M^{surf,P}$	Half-saturation constant for mineral surface PO_x adsorption	g m^{-2}	64	[*Y P Wang et al.*, 2010]
$[E_P^{plant}]$	Plant phosphorus carrier enzyme abundance for PO_x uptake	g m^{-2}	$C_{froot} \cdot 0.0000125$ (a)	[*Tang and Riley*, 2013; *Trumbore et al.*, 2006]
$[E_P^{mic}]$	Decomposing microbes phosphorus carrier enzyme abundance for PO_x immobilization	g m^{-2}	$\frac{F_P^{immob,pot}}{800}$ (b)	[*Tang and Riley*, 2013]
$[E_P^{surf}]$	Mineral surface "effective enzyme" abundance for PO_x adsorption	g m^{-2}	$VMAX_P^{surf} - [SP]$	[*Tang and Riley*, 2013]

(a) The scaling factor for plant nutrient enzyme abundance is 0.0000125. This number is inferred by assuming that growing season plant nutrient carrier enzymes are roughly the same order of magnitude compared with decomposing microbes'. Typical values for soil decomposing microbe biomass and tropical forest fine root biomass are 0.1 [*Tang and Riley*, 2013] and 400 [*Trumbore et al.*, 2006] gC m^{-2}. A typical value of scaling factor that scales microbial biomass to enzyme abundance is 0.05 [*Tang and Riley*, 2013]. Therefore, $C_{froot} \cdot x = C_{mic} \cdot 0.05$ or $400 \cdot x = 0.1 \cdot 0.05$. We have $x = 0.0000125$. Further, we have $k_{NH4}^{plant} \cdot [E_N^{plant}] = VMAX_{NH4}^{plant}$. We know that typical values for $VMAX_{NH4}^{plant}$ and $[E_N^{plant}]$ are 0.6 g m^{-2} day^{-1} [*Min et al.*, 2000] and 0.005 g m^{-2}. Then we have $k_{NH4}^{plant} = 120$ day^{-1}. Similarly, we have $k_{NO3}^{plant} \cdot [E_N^{plant}] = VMAX_{NO3}^{plant}$, $k_P^{plant} \cdot [E_P^{plant}] = VMAX_P^{plant}$. Knowing that typical values for $VMAX_{NO3}^{plant}$ and $VMAX_P^{plant}$ are 0.01 [*Min et al.*, 2000] and 0.06 [*Colpaert et al.*, 1999] g m^{-2} day^{-1}, we have $k_{NO3}^{plant} = 2$ and $k_P^{plant} = 12$ day^{-1}.

(b) For decomposing microbes, we have $VMAX_N^{mic} = k_N^{mic} \cdot [E_N^{mic}]$. Typical values for $VMAX_N^{immob}$ and $[E_N^{mic}]$ are 5 g m^{-2} day^{-1} [*Kuzyakov and Xu*, 2013] and 0.005 g m^{-2} [*Tang and Riley*, 2013]. Therefore, we have $k_N^{mic} = 1000$. Since our model calculates potential N immobilization rates and approximates them as $VMAX_N^{mic}$. The changes of potential N immobilization rates at each time step imply the changes of enzyme abundance through $[E_N^{mic}] = \frac{F_N^{immob,pot}}{k_N^{mic}} = \frac{F_N^{immob,pot}}{1000}$. Similarly, we have that $VMAX_P^{immob}$ and $[E_N^{mic}]$ are 2 g m^{-2} day^{-1} [*Chen*, 1974] and 0.005 g m^{-2}. Therefore, $k_P^{mic} = 800$ and $E_P^{mic} = \frac{F_P^{immob,pot}}{800}$.

762 **Table 3.** Observational datasets used for calibration. Number of observations for each data stream is included in brackets.

Processes	Datasets		Location	References
C associated	Soil heterotrophic respiration (20)		Tapajos National Forest, Para, Brazil	[*Silver et al.*, 2012]
N associated	Soil NH_4^+ (5)	N_2O efflux (20)	Tapajos National Forest, Para, Brazil	[*Silver et al.*, 2012]
P associated	Soil free phosphate (3)	Sorb phosphate (3)	Tapajos National Forest, Para, Brazil	[*McGroddy et al.*, 2008]

763

Table 4. Calibrated parameters are reported in terms of (1) mean/standard deviation by fitting to a Gaussian distribution; (2) 25% and 75% quantile. Both variance-based and quantile-based parameters uncertainty reduction are provided; (3) Gelman-Rubin convergence criterion.

Parameters	μ_{prior}	σ_{prior}	$\mu_{posterior}$	$\sigma_{posterior}$	**UR**	Q^{25}_{prior}	Q^{75}_{prior}	$Q^{25}_{posterior}$	$Q^{75}_{posterior}$	**UR**	**Gelman-Rubin criterion**
$TURN_{SOM}$ [CWD, metabolic, cellulose, lignin lit, fast, medium SOM]	[3.7, 0.06, 0.23, 0.23,0.16, 4.6]	[3.9, 0.06, 0.24, 0.24, 0.18, 4.8]	[5.2, 0.07, 0.17, 0.17, 0.14, 3.6]	[0.33, 0.01, 0.01, 0.005, 0.008, 0.37]	[92, 83, 96, 98, 96, 92]	[5.33, 0.086, 0.33, 0.33, 0.22, 6.5]	[19.32, 0.31, 1.18, 1.18, 0.8, 23.5]	[5.05, 0.63, 0.16, 0.17, 0.13, 3.2]	[5.39, 0.076, 0.18, 0.18, 0.14, 3.9]	[97, 94, 97, 99, 98, 96	[1.69, 1.03, 1.75, 1.01, 1.06, 1.55]
k^{plant}_{NH4}	109	114	58	14	88	156.1	565.4	52.8	60.0	98	1.87
$K^{plant,NH4}_{M}$	0.082	0.086	0.173	0.018	79	0.12	0.42	0.16	0.18	93	2.86
$K^{mic,NH4}_{M}$	0.018	0.019	0.071	0.0067	65	0.026	0.094	0.065	0.076	85	1.94
k_{nit}	0.091	0.095	0.37	0.038	60	0.13	0.47	0.36	0.39	91	2.02
$K^{nit,NH4}_{M}$	0.069	0.072	0.082	0.012	83	0.10	0.36	0.07	0.09	94	1.95
k^{plant}_{NO3}	1.8	1.9	7.6	1.7	13	2.60	9.42	6.11	9.14	56	1.01

$K_M^{plant,NO3}$	0.064	0.067	0.085	0.0064	90	0.09	0.33	0.08	0.09	97	3.17
$K_M^{mic,NO3}$	0.036	0.038	0.096	0.014	63	0.05	0.19	0.09	0.10	92	2.64
$K_M^{den,NO3}$	0.0101	0.0105	0.022	0.0034	68	0.014	0.052	0.019	0.024	87	1.03
k_P^{plant}	11	11.5	59	0.75	93	15.61	56.54	58.86	59.81	98	1.06
$K_M^{plant,P}$	0.061	0.064	0.11	0.015	77	0.09	0.32	0.10	0.12	94	1.52
$K_M^{mic,P}$	0.018	0.019	0.037	0.0047	75	0.026	0.094	0.034	0.039	93	2.86
$VMAX_P^{surf}$	121	127	182	30	76	173.0	626.6	156.5	206.3	89	2.25
$K_M^{surf,P}$	64	58	200	50	18	83.2	301.5	162.6	233.0	68	1.05

767

768 **Table 5.** Short-term (24 or 48 hours) fertilization experiments of NH_4^+, NO_3^-, or PO_4^{3-} additions used to evaluate the performance of

769 the N-COM competition scheme.

Datasets	**Added nutrient**	**Competitors**			**Duration (hour)**	**References**
PO_4^{3-} fertilization	10 μg g^{-1}	I. Mineral surface	II. Decomposing microbe		48	[*Olander and Vitousek*, 2005]
NH_4^+ fertilization	4.6 μg g^{-1}	I. Plant	II. Decomposing microbe	III. Nitrifier	24	[*Templer et al.*, 2008]
NO_3^- fertilization	0.92 μg g^{-1}	I. Plant	II. Decomposing microbe		24	[*Templer et al.*, 2008]

770

References:

Anav, A., P. Friedlingstein, M. Kidston, L. Bopp, P. Ciais, P. Cox, C. Jones, M. Jung, R. Myneni, and Z. Zhu (2013), Evaluating the land and ocean components of the global carbon cycle in the CMIP5 Earth System Models, *Journal of Climate*, *26*(18), 6801-6843.

Begum, H. H., and M. T. Islam (2005), Role of synthesis and exudation of organic acids in phosphorus nutrition in plants in tropical soils, *Biotechnology*, *4*(4), 333-340.

Bonachela, J. A., M. Raghib, and S. A. Levin (2011), Dynamic model of flexible phytoplankton nutrient uptake, *Proceedings of the National Academy of Sciences*, *108*(51), 20633-20638.

Bonan, G. B., and K. V. Cleve (1992), Soil temperature, nitrogen mineralization, and carbon source-sink relationships in boreal forests, *Canadian Journal of Forest Research*, *22*(5), 629-639.

Chauhan, B. S., J. W. B. Stewart, and E. A. Paul (1981), Effect of labile inorganic phosphate status and organic carbon additions on the microbial uptake of phosphorus in soils, *Canadian Journal of Soil Science*, *61*(2), 373-385.

Chaves, M. M., J. P. Maroco, and J. S. Pereira (2003), Understanding plant responses to drought—from genes to the whole plant, *Functional plant biology*, *30*(3), 239-264.

Chen, M. (1974), Kinetics of phosphorus absorption byCorynebacterium bovis, *Microbial ecology*, *1*(1), 164-175.

793 Cogliatti, D. H., and D. T. Clarkson (1983), Physiological changes in, and phosphate
794 uptake by potato plants during development of, and recovery from
795 phosphate deficiency, *Physiologia plantarum*, *58*(3), 287-294.
796 Colpaert, J. V., K. K. Van Tichelen, J. A. Van Assche, and A. Van Laere (1999), Short-
797 term phosphorus uptake rates in mycorrhizal and non-mycorrhizal roots of
798 intact Pinus sylvestris seedlings, *New Phytologist*, *143*(3), 589-597.
799 DeLuca, T. H., O. Zackrisson, M. J. Gundale, and M.-C. Nilsson (2008), Ecosystem
800 feedbacks and nitrogen fixation in boreal forests, *Science*, *320*(5880), 1181-
801 1181.
802 DeLuca, T. H., O. Zackrisson, M.-C. Nilsson, and A. Sellstedt (2002), Quantifying
803 nitrogen-fixation in feather moss carpets of boreal forests, *Nature*,
804 *419*(6910), 917-920.
805 Dise, N. B., and R. F. Wright (1995), Nitrogen leaching from European forests in
806 relation to nitrogen deposition, *Forest Ecology and Management*, *71*(1), 153-
807 161.
808 Drake, J. E., A. Gallet‐Budynek, K. S. Hofmockel, E. S. Bernhardt, S. A. Billings, R. B.
809 Jackson, K. S. Johnsen, J. Lichter, H. R. McCarthy, and M. L. McCormack (2011),
810 Increases in the flux of carbon belowground stimulate nitrogen uptake and
811 sustain the long‐term enhancement of forest productivity under elevated
812 CO2, *Ecology letters*, *14*(4), 349-357.
813 Drtil, M., P. Nemeth, and I. Bodik (1993), Kinetic constants of nitrification, *Water*
814 *Research*, *27*(1), 35-39.

Elser, J. J., M. E. S. Bracken, E. E. Cleland, D. S. Gruner, W. S. Harpole, H. Hillebrand, J. T. Ngai, E. W. Seabloom, J. B. Shurin, and J. E. Smith (2007), Global analysis of nitrogen and phosphorus limitation of primary producers in freshwater, marine and terrestrial ecosystems, *Ecology letters*, *10*(12), 1135-1142.

FÖHse, D., N. Claassen, and A. Jungk (1988), Phosphorus efficiency of plants: I. External and internal P requirement and P uptake efficiency of different plant species, *Plant and Soil*, 101-109.

Friedlingstein, P., P. Cox, R. Betts, L. Bopp, W. Von Bloh, V. Brovkin, P. Cadule, S. Doney, M. Eby, and I. Fung (2006), Climate-carbon cycle feedback analysis: Results from the C4MIP model intercomparison, *Journal of Climate*, *19*(14), 3337-3353.

Hobbie, J. E., and E. A. Hobbie (2006), 15N in symbiotic fungi and plants estimates nitrogen and carbon flux rates in arctic tundra, *Ecology*, *87*(4), 816-822.

Hodge, A., and A. H. Fitter (2010), Substantial nitrogen acquisition by arbuscular mycorrhizal fungi from organic material has implications for N cycling, *Proceedings of the National Academy of Sciences*, *107*(31), 13754-13759.

Hodge, A., D. Robinson, and A. Fitter (2000a), Are microorganisms more effective than plants at competing for nitrogen?, *Trends in plant science*, *5*(7), 304-308.

Hodge, A., J. Stewart, D. Robinson, B. S. Griffiths, and A. H. Fitter (2000b), Competition between roots and soil micro‐organisms for nutrients from nitrogen‐rich patches of varying complexity, *Journal of Ecology*, *88*(1), 150-164.

837 Houghton, R. A. (2003), Revised estimates of the annual net flux of carbon to the
838 atmosphere from changes in land use and land management 1850–2000,
839 *Tellus B*, *55*(2), 378-390.
840 Hu, S., F. S. Chapin, M. K. Firestone, C. B. Field, and N. R. Chiariello (2001), Nitrogen
841 limitation of microbial decomposition in a grassland under elevated CO2,
842 *Nature*, *409*(6817), 188-191.
843 Iversen, C. M., T. D. Hooker, A. T. Classen, and R. J. Norby (2011), Net mineralization
844 of N at deeper soil depths as a potential mechanism for sustained forest
845 production under elevated [CO2], *Global change biology*, *17*(2), 1130-1139.
846 Jackson, R. B., C. W. Cook, J. S. Pippen, and S. M. Palmer (2009), Increased
847 belowground biomass and soil CO2 fluxes after a decade of carbon dioxide
848 enrichment in a warm-temperate forest, *Ecology*, *90*(12), 3352-3366.
849 Jackson, R. B., H. A. Mooney, and E. D. Schulze (1997), A global budget for fine root
850 biomass, surface area, and nutrient contents, *Proceedings of the National*
851 *Academy of Sciences*, *94*(14), 7362-7366.
852 Ji, D., et al. (2014), Description and basic evaluation of Beijing Normal University
853 Earth System Model (BNU-ESM) version 1, *Geosci. Model Dev.*, *7*(5), 2039-
854 2064, doi:10.5194/gmd-7-2039-2014.
855 Johnson, D. W. (1992), Nitrogen retention in forest soils, *Journal of Environmental*
856 *Quality*, *21*(1), 1-12.
857 Kaspari, M., M. N. Garcia, K. E. Harms, M. Santana, S. J. Wright, and J. B. Yavitt (2008),
858 Multiple nutrients limit litterfall and decomposition in a tropical forest,
859 *Ecology Letters*, *11*(1), 35-43.

860 Kaye, J. P., and S. C. Hart (1997), Competition for nitrogen between plants and soil
861 microorganisms, *Trends in Ecology & Evolution*, *12*(4), 139-143.
862 Korsaeth, A., L. Molstad, and L. R. Bakken (2001), Modelling the competition for
863 nitrogen between plants and microflora as a function of soil heterogeneity,
864 *Soil Biology and Biochemistry*, *33*(2), 215-226.
865 Koven, C. D., W. J. Riley, Z. M. Subin, J. Y. Tang, M. S. Torn, W. D. Collins, G. B. Bonan, D.
866 M. Lawrence, and S. C. Swenson (2013), The effect of vertically resolved soil
867 biogeochemistry and alternate soil C and N models on C dynamics of CLM4,
868 *Biogeosciences*, *10*, 7109-7131.
869 Kuzyakov, Y., and X. Xu (2013), Competition between roots and microorganisms for
870 nitrogen: mechanisms and ecological relevance, *New Phytologist*, *198*(3),
871 656-669.
872 Lambers, H., C. Mougel, B. Jaillard, and P. Hinsinger (2009), Plant-microbe-soil
873 interactions in the rhizosphere: an evolutionary perspective, *Plant and Soil*,
874 *321*(1-2), 83-115.
875 Le Quéré, C., R. J. Andres, T. Boden, T. Conway, R. A. Houghton, J. I. House, G. Marland,
876 G. P. Peters, G. R. van der Werf, and A. Ahlström (2013), The global carbon
877 budget 1959–2011, *Earth System Science Data*, *5*(1), 165-185.
878 Le Quéré, C., M. R. Raupach, J. G. Canadell, and G. Marland (2009), Trends in the
879 sources and sinks of carbon dioxide, *Nature Geoscience*, *2*(12), 831-836.
880 LeBauer, D. S., and K. K. Treseder (2008), Nitrogen limitation of net primary
881 productivity in terrestrial ecosystems is globally distributed, *Ecology*, *89*(2),
882 371-379.

883 Li, C., J. Aber, F. Stange, K. Butterbach‐Bahl, and H. Papen (2000), A process‐
884 oriented model of N2O and NO emissions from forest soils: 1. Model
885 development, *Journal of Geophysical Research: Atmospheres (1984–2012)*,
886 *105*(D4), 4369-4384.
887 Maggi, F., C. Gu, W. J. Riley, G. M. Hornberger, R. T. Venterea, T. Xu, N. Spycher, C.
888 Steefel, N. L. Miller, and C. M. Oldenburg (2008), A mechanistic treatment of
889 the dominant soil nitrogen cycling processes: Model development, testing,
890 and application, *Journal of Geophysical Research: Biogeosciences (2005–2012)*,
891 *113*(G2).
892 Maggi, F., and W. J. Riley (2009), Transient competitive complexation in biological
893 kinetic isotope fractionation explains nonsteady isotopic effects: Theory and
894 application to denitrification in soils, *Journal of Geophysical Research:*
895 *Biogeosciences (2005–2012)*, *114*(G4).
896 Marion, G. M., P. C. Miller, J. Kummerow, and W. C. Oechel (1982), Competition for
897 nitrogen in a tussock tundra ecosystem, *Plant and soil*, *66*(3), 317-327.
898 Marland, G., T. A. Boden, R. J. Andres, A. L. Brenkert, and C. A. Johnston (2003),
899 Global, regional, and national fossil fuel CO2 emissions, *Trends: A*
900 *compendium of data on global change*, 34-43.
901 Matson, P., K. A. Lohse, and S. J. Hall (2002), The globalization of nitrogen
902 deposition: consequences for terrestrial ecosystems, *AMBIO: A Journal of the*
903 *Human Environment*, *31*(2), 113-119.

Matson, P., W. H. McDowell, A. R. Townsend, and P. M. Vitousek (1999), The globalization of N deposition: ecosystem consequences in tropical environments, *Biogeochemistry*, *46*(1-3), 67-83.

McGroddy, M. E., W. L. Silver, R. C. De Oliveira, W. Z. De Mello, and M. Keller (2008), Retention of phosphorus in highly weathered soils under a lowland Amazonian forest ecosystem, *Journal of Geophysical Research: Biogeosciences (2005–2012)*, *113*(G4).

McGuire, A. D., J. M. Melillo, L. A. Joyce, D. W. Kicklighter, A. L. Grace, B. Moore, and C. J. Vorosmarty (1992), Interactions between carbon and nitrogen dynamics in estimating net primary productivity for potential vegetation in North America, *Global Biogeochemical Cycles*, *6*(2), 101-124.

Medvigy, D., S. C. Wofsy, J. W. Munger, D. Y. Hollinger, and P. R. Moorcroft (2009), Mechanistic scaling of ecosystem function and dynamics in space and time: Ecosystem Demography model version 2, *Journal of Geophysical Research: Biogeosciences (2005–2012)*, *114*(G1).

Min, X., M. Y. Siddiqi, R. D. Guy, A. D. M. Glass, and H. J. Kronzucker (2000), A comparative kinetic analysis of nitrate and ammonium influx in two early‐successional tree species of temperate and boreal forest ecosystems, *Plant, Cell & Environment*, *23*(3), 321-328.

Moorcroft, P. R., G. C. Hurtt, and S. W. Pacala (2001), A method for scaling vegetation dynamics: the ecosystem demography model (ED), *Ecological monographs*, *71*(4), 557-586.

926 Moorhead, D. L., and R. L. Sinsabaugh (2006), A theoretical model of litter decay and
927 microbial interaction, *Ecological Monographs*, *76*(2), 151-174.
928 Mooshammer, M., W. Wanek, S. Zechmeister-Boltenstern, and A. Richter (2014),
929 Stoichiometric imbalances between terrestrial decomposer communities and
930 their resources: mechanisms and implications of microbial adaptations to
931 their resources, *Frontiers in microbiology*, *5*.
932 Murray, R. E., L. L. Parsons, and M. S. Smith (1989), Kinetics of nitrate utilization by
933 mixed populations of denitrifying bacteria, *Applied and Environmental*
934 *Microbiology*, *55*(3), 717-721.
935 Nedwell, D. B. (1999), Effect of low temperature on microbial growth: lowered
936 affinity for substrates limits growth at low temperature, *FEMS Microbiology*
937 *Ecology*, *30*(2), 101-111.
938 Norby, R. J., J. Ledford, C. D. Reilly, N. E. Miller, and E. G. O'Neill (2004), Fine-root
939 production dominates response of a deciduous forest to atmospheric CO2
940 enrichment, *Proceedings of the National Academy of Sciences of the United*
941 *States of America*, *101*(26), 9689-9693.
942 Norby, R. J., J. M. Warren, C. M. Iversen, B. E. Medlyn, and R. E. McMurtrie (2010),
943 CO2 enhancement of forest productivity constrained by limited nitrogen
944 availability, *Proceedings of the National Academy of Sciences*, *107*(45), 19368-
945 19373.
946 Nordin, A., P. Högberg, and T. Näsholm (2001), Soil nitrogen form and plant nitrogen
947 uptake along a boreal forest productivity gradient, *Oecologia*, *129*(1), 125-
948 132.

949 Olander, L. P., and P. M. Vitousek (2004), Biological and geochemical sinks for
950 phosphorus in soil from a wet tropical forest, *Ecosystems*, *7*(4), 404-419.
951 Olander, L. P., and P. M. Vitousek (2005), Short-term controls over inorganic
952 phosphorus during soil and ecosystem development, *Soil Biology and*
953 *Biochemistry*, *37*(4), 651-659.
954 Oren, R., D. S. Ellsworth, K. H. Johnsen, N. Phillips, B. E. Ewers, C. Maier, K. V. R.
955 Schäfer, H. McCarthy, G. Hendrey, and S. G. McNulty (2001), Soil fertility
956 limits carbon sequestration by forest ecosystems in a CO2-enriched
957 atmosphere, *Nature*, *411*(6836), 469-472.
958 Pappas, C., S. Fatichi, S. Leuzinger, A. Wolf, and P. Burlando (2013), Sensitivity
959 analysis of a process‐based ecosystem model: Pinpointing parameterization
960 and structural issues, *Journal of Geophysical Research: Biogeosciences*, *118*(2),
961 505-528.
962 Parton, W. J., E. A. Holland, S. J. Del Grosso, M. D. Hartman, R. E. Martin, A. R. Mosier,
963 D. S. Ojima, and D. S. Schimel (2001), Generalized model for NO x and N2O
964 emissions from soils, *Journal of Geophysical Research: Atmospheres (1984–*
965 *2012)*, *106*(D15), 17403-17419.
966 Parton, W. J., J. W. B. Stewart, and C. V. Cole (1988), Dynamics of C, N, P and S in
967 grassland soils: a model, *Biogeochemistry*, *5*(1), 109-131.
968 Perakis, S. S., and L. O. Hedin (2002), Nitrogen loss from unpolluted South American
969 forests mainly via dissolved organic compounds, *Nature*, *415*(6870), 416-
970 419.

971 Phillips, R. P., A. C. Finzi, and E. S. Bernhardt (2011), Enhanced root exudation
972 induces microbial feedbacks to N cycling in a pine forest under long‐term
973 CO2 fumigation, *Ecology Letters*, *14*(2), 187-194.
974 Potter, C. S., J. T. Randerson, C. B. Field, P. A. Matson, P. M. Vitousek, H. A. Mooney,
975 and S. A. Klooster (1993), Terrestrial ecosystem production: a process model
976 based on global satellite and surface data, *Global Biogeochemical Cycles*, *7*(4),
977 811-841.
978 Provides, G. F. W. I. (2014), Climate Model Intercomparisons: Preparing for the Next
979 Phase, *Eos*, *95*(9).
980 Raynaud, X., J.-C. Lata, and P. W. Leadley (2006), Soil microbial loop and nutrient
981 uptake by plants: a test using a coupled C: N model of plant–microbial
982 interactions, *Plant and Soil*, *287*(1-2), 95-116.
983 Raynaud, X., and P. W. Leadley (2004), Soil characteristics play a key role in
984 modeling nutrient competition in plant communities, *Ecology*, *85*(8), 2200-
985 2214.
986 Reich, P. B., and S. E. Hobbie (2013), Decade-long soil nitrogen constraint on the CO2
987 fertilization of plant biomass, *Nature Climate Change*, *3*(3), 278-282.
988 Reich, P. B., S. E. Hobbie, T. Lee, D. S. Ellsworth, J. B. West, D. Tilman, J. M. H. Knops, S.
989 Naeem, and J. Trost (2006), Nitrogen limitation constrains sustainability of
990 ecosystem response to CO2, *Nature*, *440*(7086), 922-925.
991 Reynolds, H. L., and S. W. Pacala (1993), An analytical treatment of root-to-shoot
992 ratio and plant competition for soil nutrient and light, *American Naturalist*,
993 51-70.

Ricciuto, D. M., K. J. Davis, and K. Keller (2008), A Bayesian calibration of a simple carbon cycle model: The role of observations in estimating and reducing uncertainty, *Global biogeochemical cycles*, *22*(2).

Rillig, M. C., M. F. Allen, J. N. Klironomos, N. R. Chiariello, and C. B. Field (1998), Plant species-specific changes in root-inhabiting fungi in a California annual grassland: responses to elevated CO2 and nutrients, *Oecologia*, *113*(2), 252-259.

Running, S. W., and J. C. Coughlan (1988), A general model of forest ecosystem processes for regional applications I. Hydrologic balance, canopy gas exchange and primary production processes, *Ecological modelling*, *42*(2), 125-154.

Schimel, J. P., and J. Bennett (2004), Nitrogen mineralization: challenges of a changing paradigm, *Ecology*, *85*(3), 591-602.

Schimel, J. P., L. E. Jackson, and M. K. Firestone (1989), Spatial and temporal effects on plant-microbial competition for inorganic nitrogen in a California annual grassland, *Soil Biology and Biochemistry*, *21*(8), 1059-1066.

Scholze, M., T. Kaminski, P. Rayner, W. Knorr, and R. Giering (2007), Propagating uncertainty through prognostic carbon cycle data assimilation system simulations, *Journal of Geophysical Research: Atmospheres (1984–2012)*, *112*(D17).

Shen, J., L. Yuan, J. Zhang, H. Li, Z. Bai, X. Chen, W. Zhang, and F. Zhang (2011), Phosphorus dynamics: from soil to plant, *Plant physiology*, *156*(3), 997-1005.

1016 Silver, W. L., A. W. Thompson, M. E. McGroddy, R. K. Varner, J. R. Robertson, H. S. J.D.
1017 Dias, P. Crill, and M. Keller (2012), LBA-ECO TG-07 Long-Term Soil Gas Flux
1018 and Root Mortality, Tapajos National Forest. Data set. Available on-line
1019 [http://daac.ornl.gov] from Oak Ridge National Laboratory Distributed
1020 Active Archive Center, *Oak Ridge, Tennessee, U.S.A.*,
1021 http://dx.doi.org/10.3334/ORNLDAAC/1116.
1022 Sokolov, A. P., D. W. Kicklighter, J. M. Melillo, B. S. Felzer, C. A. Schlosser, and T. W.
1023 Cronin (2008), Consequences of considering carbon-nitrogen interactions on
1024 the feedbacks between climate and the terrestrial carbon cycle, *Journal of*
1025 *Climate*, *21*(15), 3776-3796.
1026 Springate, D. A., and P. X. Kover (2014), Plant responses to elevated temperatures: a
1027 field study on phenological sensitivity and fitness responses to simulated
1028 climate warming, *Global change biology*, *20*(2), 456-465.
1029 Stocker, T. F., D. Qin, G.-K. Plattner, M. Tignor, S. K. Allen, J. Boschung, A. Nauels, Y.
1030 Xia, V. Bex, and P. M. Midgley (2013), Climate Change 2013. The Physical
1031 Science Basis. Working Group I Contribution to the Fifth Assessment Report
1032 of the Intergovernmental Panel on Climate Change-Abstract for decision-
1033 makers*Rep.*, Groupe d'experts intergouvernemental sur l'evolution du
1034 climat/Intergovernmental Panel on Climate Change-IPCC, C/O World
1035 Meteorological Organization, 7bis Avenue de la Paix, CP 2300 CH-1211
1036 Geneva 2 (Switzerland).
1037 Tang, J. Y., and W. J. Riley (2013), A total quasi-steady-state formulation of substrate
1038 uptake kinetics in complex networks and an example application to microbial

litter decomposition, *Biogeosciences*, *10*(12), 8329-8351, doi:10.5194/bg-10-8329-2013.

Tang, J. Y., and W. J. Riley (2014), Weaker soil carbon-climate feedbacks resulting from microbial and abiotic interactions, *Nature Clim. Change*, *advance online publication*, doi:10.1038/nclimate2438 http://www.nature.com/nclimate/journal/vaop/ncurrent/abs/nclimate2438.html - supplementary-information.

Templer, P. H., W. L. Silver, J. Pett-Ridge, K. M. DeAngelis, and M. K. Firestone (2008), Plant and microbial controls on nitrogen retention and loss in a humid tropical forest, *Ecology*, *89*(11), 3030-3040.

Thomas, R. Q., G. B. Bonan, and C. L. Goodale (2013a), Insights into mechanisms governing forest carbon response to nitrogen deposition: a model-data comparison using observed responses to nitrogen addition, *Biogeosciences Discussions*, *10*(1), 1635-1683.

Thomas, R. Q., S. Zaehle, P. H. Templer, and C. L. Goodale (2013b), Global patterns of nitrogen limitation: confronting two global biogeochemical models with observations, *Global change biology*, *19*(10), 2986-2998.

Thornton, P. E., J. F. Lamarque, N. A. Rosenbloom, and N. M. Mahowald (2007), Influence of carbon‐nitrogen cycle coupling on land model response to CO2 fertilization and climate variability, *Global Biogeochemical Cycles*, *21*(4).

Treseder, K. K., and P. M. Vitousek (2001), Effects of soil nutrient availability on investment in acquisition of N and P in Hawaiian rain forests, *Ecology*, *82*(4), 946-954.

1062 Trumbore, S., E. S. Da Costa, D. C. Nepstad, P. Barbosa De Camargo, L. A. Martinelli, D.
1063 Ray, T. Restom, and W. Silver (2006), Dynamics of fine root carbon in
1064 Amazonian tropical ecosystems and the contribution of roots to soil
1065 respiration, *Global Change Biology*, *12*(2), 217-229.
1066 Vitousek, P. M., and H. Farrington (1997), Nutrient limitation and soil development:
1067 experimental test of a biogeochemical theory, *Biogeochemistry*, *37*(1), 63-75.
1068 Vitousek, P. M., and R. W. Howarth (1991), Nitrogen limitation on land and in the
1069 sea: how can it occur?, *Biogeochemistry*, *13*(2), 87-115.
1070 Vitousek, P. M., S. Porder, B. Z. Houlton, and O. A. Chadwick (2010), Terrestrial
1071 phosphorus limitation: mechanisms, implications, and nitrogen-phosphorus
1072 interactions, *Ecological applications*, *20*(1), 5-15.
1073 Vitousek, P. M., and R. L. Sanford (1986), Nutrient cycling in moist tropical forest,
1074 *Annual review of Ecology and Systematics*, 137-167.
1075 Waksman, S. A. (1931), Principles of soil microbiology, *Principles of soil*
1076 *microbiology.*
1077 Walker, T. W., and J. K. Syers (1976), The fate of phosphorus during pedogenesis,
1078 *Geoderma*, *15*(1), 1-19.
1079 Wang, J., and B. Lars, R (1997), Competition for nitrogen during mineralization of
1080 plant residues in soil: microbial response to C and N availability, *Soil Biology*
1081 *and Biochemistry*, *29*(2), 163-170.
1082 Wang, Y. P., B. Z. Houlton, and C. B. Field (2007), A model of biogeochemical cycles of
1083 carbon, nitrogen, and phosphorus including symbiotic nitrogen fixation and
1084 phosphatase production, *Global Biogeochemical Cycles*, *21*(1).

1085 Wang, Y. P., R. M. Law, and B. Pak (2010), A global model of carbon, nitrogen and
1086 phosphorus cycles for the terrestrial biosphere, *Biogeosciences*, *7*(7), 2261-
1087 2282.
1088 Wieder, W. R., C. C. Cleveland, and A. R. Townsend (2009), Controls over leaf litter
1089 decomposition in wet tropical forests, *Ecology*, *90*(12), 3333-3341.
1090 Woodmansee, R. G., I. Vallis, and J. J. Mott (1981), Grassland nitrogen, *Ecological*
1091 *Bulletins (Sweden)*.
1092 Xu, X., P. E. Thornton, and W. M. Post (2013), A global analysis of soil microbial
1093 biomass carbon, nitrogen and phosphorus in terrestrial ecosystems, *Global*
1094 *Ecology and Biogeography*, *22*(6), 737-749.
1095 Yang, X., P. E. Thornton, D. M. Ricciuto, and W. M. Post (2014), The role of
1096 phosphorus dynamics in tropical forests–a modeling study using CLM-CNP,
1097 *Biogeosciences*, *11*(6), 1667-1681.
1098 Zaehle, S., and D. Dalmonech (2011), Carbon–nitrogen interactions on land at global
1099 scales: current understanding in modelling climate biosphere feedbacks,
1100 *Current Opinion in Environmental Sustainability*, *3*(5), 311-320.
1101 Zaehle, S., P. Friedlingstein, and A. D. Friend (2010), Terrestrial nitrogen feedbacks
1102 may accelerate future climate change, *Geophysical Research Letters*, *37*(1).
1103 Zaehle, S., and A. D. Friend (2010), Carbon and nitrogen cycle dynamics in the O‐
1104 CN land surface model: 1. Model description, site‐scale evaluation, and
1105 sensitivity to parameter estimates, *Global Biogeochemical Cycles*, *24*(1).
1106 Zaehle, S., B. E. Medlyn, M. G. De Kauwe, A. P. Walker, M. C. Dietze, T. Hickler, Y. Luo,
1107 Y. P. Wang, B. El‐Masri, and P. Thornton (2014), Evaluation of 11 terrestrial

carbon‐nitrogen cycle models against observations from two temperate Free‐Air CO2 Enrichment studies, *New Phytologist*, *202*(3), 803-822.

Zhang, Q., Y. P. Wang, A. J. Pitman, and Y. J. Dai (2011), Limitations of nitrogen and phosphorous on the terrestrial carbon uptake in the 20th century, *Geophysical Research Letters*, *38*(22).

Zhu, Q., and W. J. Riley (2015), Improved modelling of soil nitrogen losses, *Nature Climate Change*, *5*(8), 705-706.

Zhu, Q., and Q. Zhuang (2013), Modeling the effects of organic nitrogen uptake by plants on the carbon cycling of boreal ecosystems, *Biogeosciences*, *10*(8), 13455-13490.

Zhu, Q., and Q. Zhuang (2014), Parameterization and sensitivity analysis of a process‐based terrestrial ecosystem model using adjoint method, *Journal of Advances in Modeling Earth Systems*.